

AD-A236 223



(1) (2)

Synaptic Plasticity in Visual Cortex: Comparison of Theory with Experiment*

by
Eugene E. Clothiaux, Mark F. Bear and
Leon N Cooper

1990

Department of Physics and
Center for Neural Science
Brown University
Providence, Rhode Island 02912

DTIC
ELECTE
S D
JUN 07 1991
D

Abstract

Experiments performed over the last three decades indicate that the response properties of neurons in striate cortex of the cat can be modified by manipulating the visual experience of the animal during a critical period of postnatal development. A theory that can account for these results in a precise, quantitative fashion may yield insight into the underlying molecular mechanisms as well as make possible the use of visual cortex as a preparation for the study of the physiological basis of learning and memory storage. Such a theory has been developed in our laboratory. It allows a precise specification of theoretical equivalents of experimental situations and makes possible detailed and quantitative comparison of theory with experiment. The aim of the present effort is to provide such a comparison for what we call "classical" rearing conditions. These include normal rearing, monocular deprivation, reverse suture, strabismus, binocular deprivation, as well as the restoration of normal binocular vision after various forms of deprivation. We find quantitative agreement of theory and experiment both for equilibrium states and the kinetics by which they are reached.

DISTRIBUTION STATEMENT R
Approved for public release
Distribution Unlimited

*This work was supported in part by the Office of Naval Research (Contract #N00014-86-K-0041), the National Science Foundation (Contract #'s EET-8719102 and DIR-8720084) and the Army Research Office (Contract #DAAL03-88-K-0116).

91 6 6 059

91-01442



Experiments performed over the last three decades indicate that the response properties of neurons in striate cortex of the cat can be modified by manipulating the visual experience of the animal during a critical period of postnatal development. While these experiments do not provide detailed information about the molecular mechanisms in play during synapse modification, they can shed light on the dynamics of synaptic change that these mechanisms produce. A theory that can account for the observed dynamics may yield vital insight in the search for the underlying molecular mechanisms. In addition, the understanding such a theory might provide could make possible the use of visual cortex as a preparation for the study of various complex interactions between neurotransmitters and receptors that lead to learning and memory storage.

Such a theory has been developed in our laboratory to account for the wide variety of experience-dependent modifications that have been observed in kitten visual cortex (reviewed by Bear et al., 1987). Originally, Nass and Cooper (1975) explored a theory in which the modification of visual cortical synapses was purely Hebbian; that is, a change to a synapse was based on the multiplication of the presynaptic and postsynaptic activities and stabilization of the synaptic weights was produced by limiting modification to cortical responses below a maximum. Cooper et al. (1979) incorporated the idea that the sign of the modification should be based on whether or not the postsynaptic response is above or below a threshold, θ . Responses above the threshold lead to strengthening of the active synapses and responses below the threshold lead to weakening of the active synapses. To stabilize the synapses without having to impose external constraints on them, θ was allowed to slide as a nonlinear function of the recent history of the cell's postsynaptic response (Bienenstock, Cooper and Munro (BCM), 1982). BCM is a "single cell" theory where modifications occur at the synapses of fibers from the lateral geniculate nucleus (LGN) onto a single cortical neuron. Scofield and Cooper (1985) extended this to a network of interconnected neurons, such as that in kitten striate cortex. To incorporate the finding that some synapses may be more resistant to change than other synapses (e.g. Singer, 1977), they introduced two types of cells into the network: cells with modifiable synapses and cells with nonmodifiable synapses. The fully connected network was later

simplified by Cooper and Scofield (1988) with the introduction of a mean-field theory, which in effect replaces all of the individual intracortical connections to a cortical neuron from every other cell in the network by one set of "effective synapses" that conveys to the cell the average activity of all of the other cells in the network. Cooper and Scofield (1988) showed that the evolution of LGN-cortical synapses is similar for either a single neuron receiving only LGN input or a neuron embedded in a mean-field network.

Several other theoretical attempts have been made to model various aspects of synaptic plasticity in visual cortex (e.g. Malsburg, 1973; Pérez et al., 1975; Linsker, 1986; Miller et al., 1989). We reserve detailed comparison with these different approaches for another publication. However, we note that one crucial distinction between BCM and many other theories is the means of synaptic stabilization. In BCM this is accomplished by a dynamically varying modification threshold, whereas these other treatments (e.g. Malsburg, 1973; Pérez et al., 1975; Miller et al., 1989) require some sum over synaptic strengths to remain constant. Without entering into a discussion here of which mechanism is more plausible, we note that it becomes an important experimental issue to distinguish between these two very different mechanisms for synaptic stabilization. In addition, the BCM theory (as will be made clear below) allows for precise specification of theoretical equivalents of experimental situations allowing detailed and quantitative comparisons of theory with experiment.

The aim of the present effort is to provide such a comparison of the BCM theory with experiment for what we call "classical" rearing conditions. These include normal binocular vision, monocular deprivation, reverse suture, strabismus, binocular deprivation, as well as the restoration of normal binocular vision after various forms of deprivation. Comparisons with the various pharmacological manipulations that affect visual cortical plasticity (e.g. Greuel et al., 1987; Reiter and Stryker, 1988; Bear et al., 1990) will be considered elsewhere.

Review of Relevant Experiments

Because the literature on visual cortical plasticity is not without some controversy,



Dist	Special
A-1	

Codes

<input type="checkbox"/>
<input type="checkbox"/>

it is useful to state our understanding of the consequences of the various visual environments on visual cortical organization. The modifications of interest are those that occur in kitten visual cortex during the second postnatal month after brief (< 2 weeks) manipulations of visual experience.

1. Acquisition of orientation selectivity and binocular responsiveness during patterned binocular vision (Normal Rearing, NR).

Important characteristics of the visual responses of most neurons in adult striate cortex are that they (1) are binocular and (2) show a strong preference for contours of a particular orientation (Hubel and Wiesel, 1962). In the early literature there is some controversy concerning the acquisition of orientation selectivity in young animals. According to one extreme view, the development of this property occurs entirely postnatally and requires patterned binocular visual experience (Barlow and Pettigrew, 1971; Pettigrew, 1974). The opposing view is that this property is present in a rudimentary form at birth and elaborates even in the absence of patterned visual input (Hubel and Wiesel, 1963). We adopt the view, which has emerged in the more recent literature, that while some orientation selectivity is present in newborn animals and may improve without visual experience during the first few weeks, maturation to adult levels of specificity and responsiveness requires contour vision during the first two months of life (Barlow, 1975; Blakemore and Van Sluylters, 1975; Buisseret and Imbert, 1976; Frégnac and Imbert, 1978; Bonds, 1979; Movshon and Van Sluylters, 1981; Frégnac and Imbert, 1984; Albus and Wolf, 1984; Braastad and Heggelund, 1985). Evidently, the increase in selectivity and responsiveness can occur quite rapidly; after dark-rearing, mature response properties can develop with only 6 hours of binocular contour vision (Imbert and Buisseret, 1975; Buisseret et al., 1978; Buisseret et al., 1982).

2. Monocular deprivation (MD) after a period of normal rearing.

The synaptic connections which generate binocular, selective responses in visual cortex remain sensitive to manipulations of visual experience during the second and third postnatal months. One manipulation is the deprivation of pattern vision through one eye, usually produced by suturing the eyelid closed. This results in a loss of responsiveness

to stimulation of the deprived eye (Wiesel and Hubel, 1963; Hubel and Wiesel, 1970; Blakemore and Van Sluoyters, 1974b; Olson and Freeman, 1975; Movshon and Dürsteler, 1977). This change in cortical ocular dominance can occur very rapidly, with noticeable effects occurring in as little as 4 to 8 hours (Freeman and Olson, 1982). Recent chronic recording studies indicate that the loss of deprived eye responsiveness is not necessarily accompanied by an immediate increase in responsiveness through the open eye (Mioche and Singer, 1989). It appears, however, that eventually there is an increase in open-eye responsiveness and that cortical neurons responding to the open eye retain their original selectivity.

The effects of lid suture evidently are caused by the loss of pattern vision rather than a diminution of retinal activity per se (Blakemore, 1976). For example, diffusing contact lenses are as effective as lid suture in producing the ocular dominance shift (Wiesel and Hubel, 1963; Blakemore, 1976). It should also be noted that in spite of the lack of responsiveness, synaptic connections from the deprived eye are still physically present in cortex (Duffy et al., 1976; Kratz et al., 1976; Tsumota and Suda, 1978; Burchfiel and Duffy, 1981; Sillito et al., 1981; Freeman and Ohzawa, 1988).

3. Reverse suture (RS).

Blakemore and Van Sluoyters (1974b) first showed that if, after a period of MD, the deprived eye was opened and the formerly open eye sutured closed, then cortical neurons would become responsive to the newly opened eye and lose responsiveness to the newly closed eye. Acute studies indicated that as the ocular dominance of cortical responses shifts from one eye to the other during RS, there is never a period when a substantial number of cells can be strongly, and equally, activated by both eyes (Movshon, 1976). Indeed, recent chronic recording experiments of Mioche and Singer (1989) demonstrate that neurons lose responsiveness to the newly deprived eye before the newly opened eye shows any recovery, thereby preventing cells from showing strong binocular responses. The majority of neurons lose responsiveness within 24 hours of the RS, followed by a recovery of newly opened eye responsiveness over the next 48 to 72 hours. These experiments also indicate that as the initially deprived eye synapses to visual cortex recover,

the original orientation selectivity emerges. However, in their acute RS experiments Blakemore and Van Sluyters (1974b) and Movshon (1976) find binocular neurons with different optimal orientations in tests of the two eyes, leaving open the possibility that during recovery the initially deprived eye can acquire an optimal orientation different from its originally preferred input.

4. Strabismus (ST).

Hubel and Wiesel (1965) first showed that misalignment of the two eyes by sectioning an extraocular muscle results in a loss of binocular responsiveness. Subsequent experiments have repeatedly verified Hubel and Wiesel's results; either divergent or convergent squint produces cortical neurons that are generally responsive to one eye or the other, but not both (Yinon et al., 1975; Yinon, 1976; Ikeda and Tremain, 1977; Blakemore and Eggers, 1978; Van Sluyters and Levitt, 1980). The critical feature in producing the loss of binocularity is the lack of correlated input in the two eyes. Numerous results indicate that a loss of correlated input, either by alternating occlusion, rotating the image in one eye relative to the other eye, or producing different patterns of illumination on corresponding regions of the two retinae simultaneously, eventually leads to a loss of binocularity (Blakemore and Van Sluyters, 1974a; Blakemore, 1976; Cynader and Mitchell, 1977; Blasdel and Pettigrew, 1979).

5. Binocular deprivation (BD).

There is general agreement that the consequences of depriving both eyes of normal vision are substantially different from the effects of MD. Whereas several days of MD are sufficient to cause a functional disconnection of the deprived eye, an equivalent period of BD leaves most cortical neurons responsive to stimulation of either eye (Wiesel and Hubel, 1965). However, quantitative studies indicate that brief periods (≤ 1 week) of binocular deprivation (by placing the animals in a darkroom) produce a 50% drop in peak neuronal responsiveness to the preferred orientation and a slight broadening of orientation selectivity (Freeman et al., 1981). Longer periods of binocular deprivation lead to a further decrease in responsiveness and selectivity. (The effects of long-term binocular deprivation seemingly differ depending on whether the deprivation is produced

by suturing both eyelids or by placing the animal in complete darkness. After binocular lid suture there appears to be a loss of binocularity (Kratz and Spear, 1976; Watkins et al., 1978; Mower et al., 1981), which is not seen during dark-rearing (Freeman et al., 1981; Mower et al., 1981)).

6. Recovery from the effects of deprivation (RE).

The extent of a neuron's recovery of its normal receptive field properties during binocular vision after a period of deprivation appears to depend on the duration of the deprivation and its possible effects on eye alignment. Dark-rearing generally produces a population of cortical neurons that are poorly responsive to stimulation of either eye. Brief periods of binocular vision after weeks of dark-rearing lead to the development of substantial levels of selectivity, responsiveness and binocularity in a very short time (Buisseret et al., 1978, 1982), whereas binocular vision after prolonged periods of dark-rearing often produces cortical neurons that are responsive but not binocular (Cynader et al., 1976; Cynader, 1983). As Cynader (1983) points out, the longer periods of dark-rearing can lead to eye misalignment and the loss of correlated input when vision is restored, which is sufficient to cause a breakdown in binocularity. Similarly, if a brief period of monocular deprivation is followed by a period of patterned binocular vision, then cortical neurons can regain their binocular receptive fields (Blasdel and Pettigrew, 1978; Freeman and Olson, 1982). Binocular vision after longer periods of monocular deprivation leads to the recovery of some cortical cells' receptive field properties in the deprived eye without an attendant rise in binocularity (Hubel and Wiesel, 1970; Mitchell et al., 1977; Olson and Freeman, 1978). The lack of binocular neurons in these kittens again may be due to the development of a strabismus during the longer periods of monocular deprivation (Mitchell et al., 1977; Olson and Freeman, 1978).

In this paper we present a detailed development of the BCM theory that is able to account for these varied experimental results. This work confirms and extends previous mathematical analyses and yields predictions that should be experimentally verifiable.

METHODS

A mean-field approximation to the full complexity of visual cortex has been described previously (Scofield and Cooper, 1985; Cooper and Scofield, 1988). In this approximation, it is proposed that visual cortex (and possibly other regions of cortex) can be treated by a combination of statistical and single cell methods, allowing the evolution of some of the synapses (e.g. the LGN-cortical synapses) to be analyzed in detail. In what follows we briefly review this approach.

Consider a single cortical neuron receiving an array of LGN fibers from the left and right eyes (Figure 1). This neuron can be viewed as the "ith" cell in a highly interconnected network with both excitatory and inhibitory connections. In the mean-field approximation of this intricate network the intracortical connections to the "ith" cell are replaced by a set of synaptic weights that convey to the cell the average activity of the other cells in the network. A further simplification that we employ in this paper is to treat the mean-field connections to the cell in the adiabatic limit; that is, the mean-field connections to the "ith" cell are assumed to remain constant while the cell's LGN-cortical synapses seek their equilibrium values. According to the analysis of Cooper and Scofield (1988), this does not change the position and/or the stability properties of the equilibrium states. However, it does change the rate at which these equilibrium states are approached, thus possibly having an effect on the various rates of evolution of the synapses during simulations of the rearing paradigms presented here. Detailed analysis of these effects will be described elsewhere.

Cooper and Scofield (1988) have also shown that the LGN-cortical synaptic weight equilibrium states of the "ith" cell in the simplified adiabatic mean-field network can be obtained by a simple transformation of the equilibrium values of the synaptic weights of a single isolated cell that has only LGN input. An important consequence is that if the isolated single cell equilibrium states have negative components, the mean-field can be chosen sufficiently inhibitory to insure that the equilibrium states of the LGN-cortical synaptic weights of the "ith" cell in the mean-field are strictly positive. Thus we can treat a single isolated cortical cell whose synaptic weights are allowed to have positive

and negative values without violating biological constraints; the results obtained for the single isolated cortical cell are applicable to a cell in a mean-field network with only positive LGN-cortical synaptic weights.

1. Postsynaptic cortical cell response.

We denote the response of the single cell at time t by the scalar $c(t)$. $c(t)$ is dependent upon the LGN-cortical afferent activity $d(t)$ and the weights, or efficacy, $m(t)$ of the LGN-cortical synapses. In general, the output $c(t)$ is a non-linear function of the input $d(t)$ and the weights $m(t)$. However, we assume that there is a region of linear dependence of $c(t)$ on $d(t)$ and $m(t)$. The existence of such a linear region appears to have some experimental justification (Ohzawa and Freeman, 1986a, 1986b). Therefore, for the purposes of the present paper, $c(t)$ is written as

$$c(t) = m(t) \cdot d(t), \quad (1)$$

i.e. the sum over all of the synapses to the postsynaptic target cell of the activity of each LGN-cortical afferent fiber multiplied by the strength of the synaptic connection of that fiber with the postsynaptic target cell.

2. LGN Input.

To model the input to visual cortex that arises from the regions of the two retinae that view the same point in visual space, we assume that LGN activity is a precise mapping of retinal ganglion cell activity. (This means that a specific image results in a specific distribution of LGN activity.) Two types of LGN-cortical input are of particular interest: (1) activity elicited when visual contours are presented to the retinae ("pattern" input); and (2) activity that arises in the absence of visual contours ("noise") (Figure 2). From our point of view the important distinction between pattern and noise input is the degree of correlation that the two types of input produce in the LGN activity. For a specific input "pattern" the activity of one LGN neuron is assumed to have a precise relation to the activity of other LGN neurons, while for "noise" the activity of one LGN neuron is independent of the activity of the other LGN neurons. Differences between distinct patterns (for example, between various stimulus orientations) are mapped into different distributions of activity across the LGN. The extent to which this is a reasonable

model of a visual environment is currently under investigation (D. Sheinberg, work in progress).

It is possible that the activity of neighboring ganglion cells may be correlated in the absence of contour vision (Mastrorarde, 1983a, 1983b, 1989). These correlations are possibly important for aspects of cortical development that occur before birth (e.g. Miller et al., 1989). However, it is not necessary to incorporate these local correlations to capture the results of the postnatal deprivation experiments using the BCM theory, nor would incorporation of these correlations substantially alter the outcome of the simulations. Our work does incorporate the fact that retinal ganglion cells and LGN neurons fire action potentials spontaneously in the absence of light (Kuffler et al., 1957; Hubel and Wiesel, 1961; Barlow and Levick, 1969).

As illustrated in Figure 2, the salient features of the input environment can be modelled using a one dimensional array of LGN fibers from each eye as the input to the cortical neuron. Accordingly, apart from noise fluctuations, a specific input pattern always corresponds to the same distribution of activity across the array of LGN fibers from each eye. *The consistent and unique distribution of activity corresponding to a specific input pattern (not the actual shape of the distribution of activity) is the critical feature.* For example, in the third row of Figure 2 the pattern of LGN activity corresponding to a horizontal bar of light on the retina is represented as a unimodal distribution of activity with a peak activity on one fiber and slightly lower activities on the immediately adjacent fibers. This pattern of activity is the signature for a horizontal bar of light: each time a horizontal bar of light is imaged on the retina this same pattern of LGN activity is generated (apart from superimposed fluctuations, or "noise"); no other pattern of retinal stimulation leads to this pattern of activity. The choice of a unimodal distribution of activity is for convenience; it is in no way essential. Any distribution of activity could be chosen to represent a horizontal bar of light, as long as 1) this distribution occurs whenever a horizontal bar of light is on the retina and 2) this distribution differs from that arising when bars of other orientations are presented.

Activity along an array of N_{g1} fibers is represented as a vector in an N_{g1} -dimensional

space. For example, the array of LGN-cortical input fiber activity from the left eye at time t is written as a single vector $\mathbf{d}^l(t)$. (As a rule, symbols appearing in bold face represent vectors and symbols appearing in plain type represent scalars. Bold face symbols that are italicized represent vectors that have both a left and right eye component; the left and right eye components are designated by the superscripts l and r , respectively.) The array of synaptic weights formed by the LGN-cortical fibers from the left eye to the neuron is denoted by the vector $\mathbf{m}^l(t)$. The j^{th} component $d_j^l(t)$ of the vector $\mathbf{d}^l(t)$ is a scalar representing the fiber activity of one (the j^{th}) left eye LGN-cortical afferent; the j^{th} component $m_j^l(t)$ of the vector $\mathbf{m}^l(t)$ is a scalar representing one (the j^{th}) left eye LGN-cortical afferent synaptic weight. For the corresponding right eye quantities we have the vectors $\mathbf{d}^r(t)$ and $\mathbf{m}^r(t)$ with components $d_j^r(t)$ and $m_j^r(t)$, respectively. Therefore, the total input to the cell with synapses $\mathbf{m}(t) = (\mathbf{m}^l(t), \mathbf{m}^r(t))$ at time t is $\mathbf{d}(t) = (\mathbf{d}^l(t), \mathbf{d}^r(t))$.

Input to the simulated neuron at time t , i.e. $\mathbf{d}(t) = (\mathbf{d}^l(t), \mathbf{d}^r(t))$, is measured with respect to the average spontaneous activity of each of the LGN-cortical fibers. For example, the input from the left eye at time t to the j^{th} synapse of the simulated cortical neuron is

$$d_j^l(t) = d_{s,j}^l(t) - d_{s,j}^l, \quad (2)$$

where $d_{s,j}^l(t)$ is the actual firing frequency and $d_{s,j}^l$ is the average spontaneous activity of the j^{th} left eye LGN afferent fiber. For simplicity, we assume that $d_{s,j}^l$ is independent of time, the eye and the fiber; that is, $d_{s,j}^l = d_{s,j}^r = d_s$ for all of the LGN fibers at each time t . Therefore,

$$d_j^l(t) = d_{s,j}^l(t) - d_s \quad (3a)$$

and

$$d_j^r(t) = d_{s,j}^r(t) - d_s. \quad (3b)$$

The corresponding vector equation for all of the fibers is

$$\mathbf{d}(t) = \mathbf{d}_s(t) - \mathbf{d}_s, \quad (4)$$

which implies that

$$\mathbf{d}^l(t) = \mathbf{d}_s^l(t) - \mathbf{d}_s^l \quad (4a)$$

for the left eye fibers and

$$\mathbf{d}^r(t) = \mathbf{d}_s^r(t) - \mathbf{d}_s^r \quad (4b)$$

for the right eye fibers.

During simulations of binocular or monocular deprivation, we assume that the deprived eyes are receiving noise input. For example, to model noise input to the left eye (the right eye would be exactly the same) assume that $d_{a,j}^1(t)$ fluctuates randomly around d_s , implying that $d_j^1(t)$ fluctuates around 0. We call these fluctuations of $d_j^1(t)$ around 0 "noise" and label them $n_j^1(t)$. The input to the cortical neuron in the absence of patterned activity is then simply

$$d_j^1(t) = n_j^1(t) \quad (5)$$

for the j^{th} fiber of the left eye (Tables 1 and 2).

In normal rearing or monocular deprivation the open eyes of the animal are constantly viewing regularly shaped objects, which are assumed to give rise to correlated patterns of LGN activity. For example, left eye contour vision of a specific object gives rise to a pattern of LGN-cortical fiber activity which we label by $d_a^{\omega,j}(t) = d_s^{\omega,j}$, where the ω represents a particular pattern of correlated activity corresponding to a specific visual stimulus at time t . Now the input to the j^{th} left eye synapse of the neuron, $d_j^1(t)$, measures the departure of $d_{a,j}^1(t) = d_{a,j}^{\omega,j}$ from the spontaneous rate d_s :

$$d_j^1(t) = d_{a,j}^1(t) - d_s = d_{a,j}^{\omega,j} - d_s. \quad (6)$$

Note that even though $d_{a,j}^{\omega,j}$ is positive, $d_j^1(t)$ may have positive and negative values. Since in an actual visual environment there generally will be random fluctuations in $d_j^1(t)$ for multiple presentations of the same visual stimulus labelled by ω , we add a noise term to the input which we again call $n_j^1(t)$ (Tables 1 and 2):

$$d_j^1(t) = d_{a,j}^{\omega,j} - d_s + n_j^1(t). \quad (7a)$$

Defining $d_j^{\omega,j} = d_{a,j}^{\omega,j} - d_s$, the input to the j^{th} left eye synapse of the neuron for the pattern labelled by ω presented at the time t becomes

$$d_j^1(t) = d_j^{\omega,j} + n_j^1(t). \quad (7b)$$

These are the "patterns" presented during the developmental portion of the simulations; for "tests" of responses the noiseless patterns $d_j^{\omega,l}$ are presented to the cell. With the same arguments for the right eye, a normal, binocular viewing experience at some time t leads to a specific correlated pattern of activity $d^{\omega} = (d^{\omega,l}, d^{\omega,r})$ with noisy fluctuations $n(t) = (n^l(t), n^r(t))$, so that

$$d(t) = (d^l(t), d^r(t)) = (d^{\omega,l} + n^l(t), d^{\omega,r} + n^r(t)). \quad (8)$$

3. Synaptic modification.

Synaptic modification is governed by the rules of the BCM theory. According to BCM, modification of the j^{th} synaptic junction at time t ($dm_j(t)/dt$) is proportional to the product of the input activity of the j^{th} left eye LGN-cortical fiber ($d_j(t)$) and a function ϕ which is defined in terms of the postsynaptic response.

The behavior of ϕ at two values of the postsynaptic response is particularly important (Figure 3A). The first is the average postsynaptic cortical cell activity due to the spontaneous firing of action potentials in the presynaptic LGN-cortical afferent fibers. (Note that we are assuming that the cortical cell spontaneous activity is due entirely to LGN-cortical input, thereby neglecting network effects.) Recall that the average level of this activity is dependent on d_s for each LGN fiber of each eye. Letting $d_s = (d_s^l, d_s^r)$ represent the spontaneous activity of all of the incoming LGN fibers to the cell, the average "spontaneous" activity of the postsynaptic neuron is (Tables 1 and 2)

$$c_s(t) = m(t) \cdot d_s = m^l(t) \cdot d_s^l + m^r(t) \cdot d_s^r. \quad (9)$$

$c_s(t)$ serves as the baseline for measuring the impact of the current LGN-cortical afferent fiber activity on the prevailing state of the postsynaptic cell. If the LGN-cortical afferent fiber activity goes above its average spontaneous level, the postsynaptic cell is depolarized compared to its average "spontaneous" state. On the other hand, if the LGN-cortical afferent fiber activity drops below its average spontaneous level, the postsynaptic cell is hyperpolarized compared to its average "spontaneous" state. This departure of the postsynaptic response from its average "spontaneous" state is the measure of the

postsynaptic cell response in the model. The ϕ function is zero at $c_s(t)$ with a negative slope (ϵ_0) at postsynaptic response levels above $c_s(t)$.

The second important level of postsynaptic cell response occurs at a value designated by $c_s(t) + \theta$. Here ϕ changes sign from negative to positive with a positive slope (ϵ_θ). According to the BCM theory, the value of θ changes as a power (larger than one) of some measure of the average postsynaptic response. This important feature of θ insures the boundedness of the synaptic weights without placing artificial constraints on them and guarantees that $\theta \geq 0$. Therefore, the threshold defined by $c_s(t) + \theta$ is never at a level of postsynaptic response lower than $c_s(t)$. Furthermore, when all of the synaptic weights approach 0 and $c_s(t) \approx 0$ for all t , θ must also eventually approach 0, thereby allowing for the possible recovery of synaptic strength.

For synaptic modification the departure of the postsynaptic cell response from $c_s(t)$ is the measure of interest. Therefore, we define

$$c(t) = c_a(t) - c_s(t), \quad (10)$$

where

$$c_a(t) = \mathbf{m}(t) \cdot \mathbf{d}_a(t) \approx \mathbf{m}^l(t) \cdot \mathbf{d}_a^l(t) + \mathbf{m}^r(t) \cdot \mathbf{d}_a^r(t), \quad (10a)$$

which is equivalent to

$$c(t) = \mathbf{m}^l(t) \cdot \mathbf{d}^l(t) + \mathbf{m}^r(t) \cdot \mathbf{d}^r(t). \quad (11)$$

To incorporate non-LGN input to the cell that is independent of the LGN input a noise term is added to $c(t)$:

$$c(t) = \mathbf{m}^l(t) \cdot \mathbf{d}^l(t) + \mathbf{m}^r(t) \cdot \mathbf{d}^r(t) + c_{\text{noise}}(t), \quad (12)$$

where $c_{\text{noise}}(t)$ is assumed to be uniformly, randomly distributed about 0 (Tables 1 and 2). Thus, for ϕ the two important values of postsynaptic response are at $c(t) = 0$ and $c(t) = \theta$. The BCM rule for synaptic modification can now be written (Tables 1 and 2):

$$\frac{d\mathbf{m}(t)}{dt} = \eta \phi(c(t), \theta(t)) \mathbf{d}(t), \quad (13)$$

where ϕ is a function such that

$$\phi(c = 0, \theta) = \phi(c = \theta, \theta) = 0 \quad (13a)$$

and the slope of ϕ at c greater than zero (ϵ_0) is negative and the slope of ϕ at $c = \theta$ (ϵ_θ) is positive (Figure 3B). The factor η , which we call the modification "step size," is a positive constant that determines the magnitude of the synaptic modification at each iteration.

One of the most striking characteristics of the BCM theory is the moving threshold. It is this moving modification threshold that provides the stability of the system. This contrasts with other synaptic modification proposals such as that of Malsburg (1973), Pérez et al. (1975) and Miller et al. (1989), where stability is produced by the requirement that some sum over the strengths of the synapses be constant.

In their original paper BCM (1982) chose as a candidate for θ the average value of the postsynaptic firing rate:

$$\theta(t) = \left(\frac{\overline{c(t)}}{c_0} \right)^p, \quad (14)$$

where $\overline{c(t)}$ represents a time average of the departure of the postsynaptic firing rate from its spontaneous level, i.e.

$$\overline{c(t)} = \frac{1}{\tau} \int_{-\infty}^t c(t') e^{-\frac{(t-t')}{\tau}} dt', \quad (14a)$$

p sets the degree of nonlinearity ($p > 1$), and c_0 is a normalization constant. This produced a workable system with the desired stability properties. However, the precise value of p and the interpretation of the cell response remained open. For example, should one use the actual firing rate of the cell or the average depolarization of the postsynaptic dendrite? If one used the average depolarization, was the appropriate quantity the total depolarization or its deviation from its spontaneous level. Such questions remain unanswered because no experiments exist to fully distinguish between their consequences.

However, recent experimental innovations, such as the chronic recording technique developed by Mioche and Singer (1988), now place us in a position to investigate much more closely several key features of the moving threshold. Consider two: (1) How rapidly does the moving threshold adjust to changes in the cell response brought on by a manipulation of the visual environment? And (2) How should the time averaging (represented by the double bars) and the nonlinearity p relate to each other?

Addressing the second question first, BCM (1982) time averaged the cell response first and then raised the time average to the power p . Recent work (Intrator, 1990) indicates that a θ based on a time average of the squared cell response, i.e.

$$\theta(t) = \overline{c(t)^p} \quad (15)$$

with $p = 2$, has some useful mathematical properties; this form also appears to produce an evolution of the synapses in agreement with the experimental results discussed in the present work.

With regard to the first question, the two elements that control the rate at which θ moves are τ and the feature of the cell response that sets θ . As τ goes to infinity (i.e. as the memory of the time average goes to infinity), the threshold adjusts more slowly to changes in the cell response. Therefore, if θ is high and the cell response suddenly drops, then for large τ , the threshold, θ , drops slowly to a level consistent with the prevailing cell response.

The exact feature of the cell response that should be used to set θ is not known at present. However, inspection of Eq. 10 does provide two distinct possibilities: 1) the total response of the cell (c_a); or 2) the original BCM choice: the deviation of the cell response from its spontaneous level (c). This distinction is important since a θ dependent on c is much more sensitive to changes in the environment than a θ dependent on c_a . When no patterns are present in the input (Eq. 5), $c(t) \approx 0$ on average, whereas $c_a(t) \approx m(t) \cdot d_a$ on average. In this situation, after the first τ iterations, θ based on c is near 0, whereas θ based on c_a is at some positive level. If θ was nonzero at the start of the simulation, then the percentage change for θ dependent on c is much larger than the percentage change for θ dependent on c_a . All of the key features of θ that are currently unspecified provide a rich area for further investigation.

In this paper we choose θ to be

$$\theta(t) = \left(\frac{\overline{c_a(t)}}{c_0} \right)^p, \quad (16)$$

where

$$c_a(t) = m(t) \cdot d_a(t) \quad (16a)$$

is the actual cell response, the double bar as usual represents a time average of the underlying quantity, i.e.

$$\overline{c_a(t)} = \frac{1}{\tau} \int_{-\infty}^t c_a(t') e^{-\frac{(t-t')}{\tau}} dt', \quad (16b)$$

and c_0 is again a normalization constant (Tables 1 and 2). With this choice of θ we are able to model the classical deprivation experiments described above.

4. Simulations.

The visual deprivation experiments we attempt to model are NR, MD, RS, ST, BD and RE. Each of the experimental paradigms can be simulated with some combination of two types of input to the two eyes: noise, i.e. $\mathbf{n}^l(t)$ and $\mathbf{n}^r(t)$, and patterns with noise superimposed, i.e. $\mathbf{d}^{\omega,l} + \mathbf{n}^l(t)$ and $\mathbf{d}^{\omega,r} + \mathbf{n}^r(t)$ ($1 \leq \omega \leq N_p$).

For example, during NR the input for the two eyes at time t is assumed to be patterned for each eye and correlated between the two eyes with each pattern of activity having the same probability of occurring:

$$d_j^l(t) = d_j^{\omega,l} + n_j^l(t) \quad (17a)$$

and

$$d_j^r(t) = d_j^{\omega,r} + n_j^r(t), \quad (17b)$$

where ω is chosen randomly from the set of N_p patterns at each iteration and $n_j^l(t)$ and $n_j^r(t)$ are independent, but statistically equivalent, noise terms. MD is similar to NR except that patterned activity is absent from the eye (left) simulated as closed:

$$d_j^l(t) = n_j^l(t) \quad (18a)$$

and

$$d_j^r(t) = d_j^{\omega,r} + n_j^r(t). \quad (18b)$$

RS is accomplished by changing the eye that is closed after an initial period of MD. Therefore, if for the initial period of MD the left eye is closed, then for RS the input is

$$d_j^l(t) = d_j^{\omega,l} + n_j^l(t) \quad (19a)$$

and

$$d_j^r(t) = n_j^r(t), \quad (19b)$$

which corresponds to the right eye closed. BD is simulated by a total lack of patterned input to the two eyes:

$$d_j^l(t) = n_j^l(t) \quad (20a)$$

and

$$d_j^r(t) = n_j^r(t). \quad (20b)$$

Finally, in a simulation of ST patterns are input to both eyes, but the patterns are uncorrelated:

$$d_j^l(t) = d_j^{\omega,l} + n_j^l(t) \quad (21a)$$

and

$$d_j^r(t) = d_j^{\omega',r} + n_j^r(t), \quad (21b)$$

where ω and ω' are independently and randomly chosen from the set of N_p patterns at each time step.

With this choice of the set of patterned and noise inputs and the synaptic modification rule the sequence of events in a simulation of any experimental paradigm is relatively straightforward (Saul and Clothiaux, 1986). First, at each step $t - dt$ to t a pattern of activity $d(t)$ is generated that represents the activity of the LGN-cortical afferents during the interval dt . The activity assignments to $d(t)$ must be consistent with the particular visual experience paradigm that is being simulated. Once the vector $d(t)$ is constructed, the resulting cell response $c(t)$ is calculated according to Eq. 12 and $dm(t)/dt$ is then determined according to Eq. 13. The whole process is repeated until the synaptic weights $m(t)$ reach equilibrium.

The dynamics of the evolution of the cell response tuning curve to its final equilibrium value is the information of interest. To follow the change in cell response selectivity and ocular dominance during a simulation, the modification process is periodically interrupted in order to assess the synaptic weight vector $m(t)$. With a record of $m(t)$ at

various intervals during the simulation, a history of the changes in cell response selectivity and ocular dominance can be easily reconstructed. The cell responses generated by stimulation of the left and right eyes separately with all N_p of the noiseless input patterns $\mathbf{d}^{\omega,l}$ and $\mathbf{d}^{\omega,r}$, respectively, are taken to be the "tuning curves" of the two eyes:

$$\text{Left Eye Tuning Curve}(t) = \{c^{l,\omega}(t) = \mathbf{m}^l(t) \cdot \mathbf{d}^{\omega,l} \mid \omega = 1, \dots, N_p\} \quad (22a)$$

$$\text{Right Eye Tuning Curve}(t) = \{c^{r,\omega}(t) = \mathbf{m}^r(t) \cdot \mathbf{d}^{\omega,r} \mid \omega = 1, \dots, N_p\}. \quad (22b)$$

Since patterns labelled by ω and $\omega + 1$ are most similar in their distribution of activity across the LGN-cortical afferents, plotting $c^{l,\omega}(t)$ and $c^{r,\omega}(t)$ versus ω (in ascending order) leads to graphs that are interpreted as analogous to visual cortical neuron response curves obtained experimentally by presenting a light bar across the retina at different orientations.

In this paper a single set of parameters is used to model the kitten visual deprivation experiments. This choice of parameters leads to an evolution of the synapses in agreement with experiment. In the discussion the effects of changing the parameters on the evolution of the synapses are considered in more detail.

RESULTS

A primary motivation for the original BCM theory was to account for the acquisition of selectivity by cortical neurons in a normal patterned environment. How this comes about is illustrated by the simulation in Figure 4. At the beginning of the simulation the LGN-cortical synaptic weights start with random values between 0 and 0.15. Since there is no bias in the synaptic weights, all of the input patterns initially produce a small cell response that may be either slightly above or below θ . During training, when the various patterns are presented at random to the cell, the synaptic weights associated with positive input activity ($d_j > 0$) strengthen when the response goes above θ (implying $\phi > 0$) because according to Eq. 13 $dm_j/dt = \eta \phi d_j$ and $\eta \phi d_j > 0$ (Figure 5). On the other hand, the synaptic weights associated with high input activity ($d_j > 0$) when the postsynaptic response fails to reach θ (implying $\phi < 0$) weaken. As pointed out by Bienenstock et al. (1982), this results in competition between patterns of activity with the consequence that the synapses that consistently participate in the activation of the cell above θ increase in strength, while the synapses whose activity fails to correlate with target activation beyond θ decrease in strength.

Growth in the cell response to some of the input patterns leads to an increase in θ , decreasing the likelihood of further increases in synaptic strength. Eventually, θ becomes large enough to stabilize the synaptic weights; that is, for θ sufficiently large the average change to the synaptic weights over all of the input patterns is 0 and the cell response to any particular pattern no longer changes significantly. Notice that this stability is dynamic: for each iteration of the simulation there are small changes in the synaptic weights; over many iterations, however, the changes to the weights average to 0.

The format of Figure 4 is used to illustrate the results of the various simulations in Figures 6 through 13. The x axis labeled by "stimulus 'orientation'" represents the different patterns in the testing set and the vertical y axis represents the response of the cell to these patterns. The z axis of the graph represents time or, more precisely, the number of iterations. The evolution of the cell's tuning curve is illustrated by the plot of "cell response" versus "stimulus 'orientation'" at each iteration. As Figure 4 shows,

presentation of patterned input to a cell quickly leads to robust responses to a select number of the input patterns. Since θ adjusts to changes in the cell response, the peak cell response eventually stabilizes at some nonzero value. (This value depends on various parameters, such as p , c_0 and τ .)

1. Normal Rearing (NR)

The NR simulation starts from poorly developed left and right eye synapses (i.e. random values between 0 and 0.15). The input to the two eyes is taken to be correlated patterns with noise superimposed (Eq. 17). As expected, the cell acquires responsiveness and selectivity (Figure 6). With a growing cell response, θ increases and eventually stabilizes the synaptic weights. Notice that the cell becomes selective to the same input patterns through the LGN-cortical fibers from each eye; this is because the left and right eye patterns are identical at each iteration, apart from noise. Although we assume no initial orientation preference, if some orientation preference is present initially, the cell will almost certainly become selective to this orientation.

As discussed before, the value of τ determines the rate at which θ moves. The rate at which θ moves in turn affects the choice of a modification step size η . The modification step size η (Eq. 13) must stay below an upper bound that is a function of the memory τ (Eq. 16b). As τ increases, implying a longer memory of $\overline{c_a(t)}$ in the calculation of θ , the upper bound on η decreases. If η is too large for a given value of τ , then the modification threshold θ cannot adjust rapidly enough to stop initial large increments in the cell response. When θ finally does increase, it over compensates and drives the cell response back to zero. The synaptic weights and threshold oscillate in an unrealistic manner. Thus we are restricted to a domain of τ and η that leads to an acceptable evolution of the system.

Once τ and η are fixed at values that lead to a realistic evolution of the synaptic weights, the next important parameter that affects the outcome of the NR simulation is the normalization constant c_0 which is used in the calculation of the value of θ (Eq. 16). c_0 sets the level of θ with respect to the initial cell response. For example, as c_0 increases, θ decreases and the cell's initial responses have a higher probability of going

above θ ; hence, the synaptic weights have a higher probability of initially increasing in strength. Notice also that increasing c_0 causes the system to stabilize at higher synaptic weights.

Finally, the magnitude of the nonlinearity p must be set. The only stringent criterion that p must satisfy is $p > 1$. In most of our work we set $p = 2$. This produces a sizable nonlinearity that leads to an acceptable evolution of the system. Generally, as p increases, θ moves more rapidly as the average cell response changes; therefore, increasing the value of p leads to smaller stabilized synaptic weights during NR.

2. Monocular Deprivation (MD)

After the period of NR has driven $m(t)$ to a stable, selective state, the simulation of MD begins by "closing the left eye." That is, the input to the left eye loses its patterned component while the right eye does not (Eq. 18). As Figure 7 illustrates, the newly closed eye LGN-cortical synapses immediately begin to drop in strength with a consequent loss of closed eye response. After the closed eye input is almost completely ineffectual in evoking a response, the open eye actually increases in efficacy and eventually stabilizes at an enhanced level; the amount of this open eye enhancement is sensitive to the choice of parameters.

The immediate drop in the cell response after the onset of MD causes a gradual drop in θ . However, θ remains far from 0 after its initial drop because the open eye input remains effective in driving the cell. When θ is high and the total postsynaptic response is near 0, the closed eye LGN-cortical synapses receiving "noise" input decrease in strength. During MD, the postsynaptic response is near 0 whenever the open eye is presented a non-preferred pattern. On the other hand, when the total postsynaptic response is near θ , as would occur when a preferred pattern is shown to the open eye, the closed eye LGN-cortical synapses receiving "noise" input actually increase in synaptic strength. Therefore, during MD, the ratio of preferred to non-preferred open eye patterns determines whether the closed eye synaptic weights increase or decrease in strength. (This effect was analyzed by BCM; a detailed treatment is given in the appendix).

The relationship between open eye selectivity and the evolution of the closed eye

synaptic weights is an integral feature of BCM (1982). To illustrate this aspect of the theory in more detail consider N consecutive iterations of the simulation, where N is much greater than the number of patterns in the training set but much less than the number of iterations necessary for a significant change in the synaptic weights. For those iterations for which non-preferred patterns are presented to the open eye so that the cell response is close to 0 (N_0 in number), the average change to the j^{th} closed eye synapse is

$$\overline{\frac{dm_j^1(t)}{dt}} \approx \eta(\epsilon_0) \overline{n^2} m_j^1(t), \quad (23a)$$

where ϵ_0 is the slope of ϕ at the origin and $\overline{n^2}$ represents the average of the square of the noise input to the j^{th} left eye fiber. On the other hand, for all of those iterations for which preferred patterns are presented to the open eye so that the cell response is close to θ (N_θ in number), the average change to the j^{th} closed eye synapse is

$$\overline{\frac{dm_j^1(t)}{dt}} \approx \eta(\epsilon_\theta) \overline{n^2} m_j^1(t), \quad (23b)$$

where ϵ_θ is the slope of ϕ at θ and $\overline{n^2}$ again represents the average of the square of the noise input to the j^{th} left eye fiber. Combining Eq. 23a and Eq. 23b, and setting $\epsilon_\theta = -\epsilon_0 = \epsilon$ for simplicity, the average change to the j^{th} closed eye synaptic weight during each of the N iterations is

$$\overline{\frac{dm_j^1(t)}{dt}} \approx \eta \left(\frac{N_\theta - N_0}{N} \right) \epsilon \overline{n^2} m_j^1(t), \quad (23c)$$

which has the solution

$$m_j^1(t) \approx m_j^1(0) e^{\eta \left(\frac{N_\theta - N_0}{N} \right) \epsilon \overline{n^2} t}, \quad (24)$$

where $m_j^1(0)$ is the synaptic strength at the beginning of the MD (see Figure 8 and the appendix). Therefore, the relative number of optimal to nonoptimal cell responses through stimulation of the open eye determines whether the closed eye synaptic weights increase or decrease. For a selective set of LGN-cortical synapses $N_\theta \ll N_0$; therefore, the closed eye synaptic weights go to 0 during MD if the cell is selective. This is the source of the correlation between ocular dominance and selectivity during MD.

As Eq. 24 indicates, the rate of disconnection of the closed eye during MD also depends on η , ϵ and the level of the noise to the closed eye ($\overline{n^2}$). Since η and ϵ are set to provide appropriate behavior for NR, the ratio of optimal to nonoptimal open eye patterns and the level of the closed eye noise are the only remaining quantities that can be varied during MD. One has the nonintuitive, experimentally testable prediction that higher levels of noise lead to a faster disconnection of the closed eye synapses, while broadening of cortical orientation selectivity slows the disconnection of the closed eye synapses.

The open eye synaptic weights eventually increase during MD because the initial drop in θ is large enough to bias the cell response to open eye patterned input toward the positive region of ϕ above θ . Therefore, the open eye efficacy goes up until it drives θ sufficiently high to stop further increases in the synaptic weights. The amount of this increase is sensitive to the choice of parameters.

3. Reverse Suture (RS)

Following a period of MD, RS consists of closing the open eye and opening the closed eye. For the simulation, if the MD input is given by Eq. 18, then for RS the input is switched to Eq. 19. With such a change of the input to the simulated cortical cell, the newly closed eye LGN-cortical synaptic weights immediately begin to weaken (Figure 9). After the newly closed eye is almost completely disconnected, the newly opened eye finally begins to show a recovery. As the newly opened eye continues to recover, the newly closed eye synapses are eventually driven to 0.

The evolution of the synaptic weights at the beginning of a RS simulation depends critically on the behavior of θ . In this simulation θ remains high at the beginning of the RS for a relatively long time. During this time the newly closed eye synapses are receiving noise and the newly opened eye synapses are weak and ineffective in driving the cell. Therefore, the newly closed eye synapses initially weaken at a rate governed by Eq. 24 with $N_\theta = 0$. Furthermore, the newly opened eye synapses cannot recover initially since they are unable to produce responses above θ for any of the input patterns. As the simulation proceeds, θ eventually drops low enough for the poor open eye responses to

exceed it and the open eye begins to recover. At this point the closed eye has almost no influence on the cortical cell.

If θ drops slowly at the beginning of a RS simulation, then the preceding argument indicates that the closed eye synapses always weaken before the open eye recovers. However, if θ were to drop quickly, the closed eye would not weaken until the open eye had recovered and θ had increased. Mioche and Singer (1989) find that the previously closed eye always weakens before the newly opened eye recovers. These results indicate that θ should not drop too quickly at the beginning of a RS.

4. Strabismus (ST)

Suppose that after a period of NR, the two eyes become strabismic. The moment the input to the two eyes becomes uncorrelated (Eq. 21) in a simulation, the eye that has the dominant input to a cortical cell holds the cell in a winner take all situation (Figure 10). The weaker eye becomes completely disconnected on a timescale comparable to monocular deprivation. Note that the results of a ST simulation do not depend critically on any of the parameters. As long as the input is given by Eq. 21, there are no binocular, stable, selective equilibrium states; the only stable, selective equilibrium states are monocular. This result does not depend on the initial state.

5. Binocular Deprivation (BD)

For BD after NR the starting point is the stable, selective equilibrium state of $m(t)$ that developed during the prior period of NR. The important aspect of the input for binocular deprivation is that it does not contain patterns of correlated activity (Eq. 20). Once the correlated activity is removed from the input, the cell's responsiveness immediately drops. The loss in responsiveness during BD leads to a weakening of the synaptic weights; however, on the same timescale as MD the drop in the weights during BD is not as precipitous (Figure 11). On a longer timescale, however, the average responsiveness to stimulation of both eyes is reduced to low levels whose exact value is dependent on the parameters (Figure 12). Further, the original orientation tuning of the cell is completely lost. Thus, unless there were a built-in preference, due perhaps to innate non-modifiable synapses or network effects, the return of patterned input could

lead to selectivity to a different orientation.

When BD begins, the situation for both eyes' LGN-cortical synapses is similar to the newly closed eye's synapses on the cortical cell during the initial stages of a RS. In both cases there are LGN-cortical fibers carrying noise at a time when the cell response is always low and θ is high. Therefore, during the initial stages of BD after NR, Eq. 24 with $N_\theta = 0$ is applicable to the synapses of both eyes and both sets of closed eye synaptic weights start dropping. Since there is no patterned input to keep θ high, however, θ also starts to drop, causing N_θ to increase from 0 and thereby slowing down the rate of decrease of the synaptic weights.

The final state of the synapses depends critically on the average value of the noise along each fiber (\bar{n}), the average level of the noise fluctuations along each fiber ($\overline{n^2}$) and the level of the postsynaptic noise $c_{\text{noise}}(t)$. When $\bar{n} = 0$ and θ is nonzero, the only equilibrium state for the system is at $\mathbf{m}(t) = 0$. However, when θ eventually approaches 0 in response to $\mathbf{m}(t)$ going to 0, the synapses start undergoing a random walk that takes $\mathbf{m}(t)$, and hence θ , away from their respective origins. The degree to which $\mathbf{m}(t)$ departs from the origin depends on the magnitude of $\overline{n^2}$ and the amplitude of the postsynaptic noise $c_{\text{noise}}(t)$. As both $\overline{n^2}$ and the amplitude of $c_{\text{noise}}(t)$ increase, thereby increasing the scatter of the cell response about its spontaneous level, the random walk around the origin becomes more noticeable in the sense that $\mathbf{m}(t)$ can spend more time further from the origin.

For $\bar{n} \neq 0$ the synaptic weight vector $\mathbf{m}(t)$ is not constrained to remain at the origin on average. As \bar{n} departs from 0, simulations and preliminary analyses suggest that a number of equilibrium states appear whose distance from the origin increases as the magnitude of \bar{n} increases. These points are usually, but not always, unselective with respect to the original set of training patterns used during NR. Further, for reasonable values of \bar{n} , the cell's response remains poor as compared to its NR levels. These results were obtained using Eq. 16 for θ ; further investigation is required to determine the evolution of $\mathbf{m}(t)$ for $\bar{n} \neq 0$ and different forms of θ .

In the current simulation $\bar{n} = 0$. Therefore, the average value for $\mathbf{m}(t)$ is the origin.

Since the amplitude of $c_{\text{noise}}(t)$ is high, $m(t)$ fluctuates noticeably around the origin with a loss of its original selectivity (Figure 12).

6. Recovery from the effects of deprivation (RE)

Recovery after a period of monocular deprivation is simulated by changing the input to the cell to that of NR. In this case the eye that was closed during the MD regains the response properties that it acquired during the initial period of NR (Figure 13). However, if the two eyes are assumed to have become misaligned during the period of MD, then during the recovery period the input must be given by Eq. 21. Uncorrelated input to a cell that is already completely shifted to one eye does not produce any significant changes and the initially deprived eye never recovers. Since strabismus is sometimes a result of MD, this may explain why recovery of normal binocularity is sometimes, but not always, observed.

As already mentioned, the loss of binocularity during uncorrelated patterned input to the two eyes is not strongly dependent on any of the parameter settings and is solely due to a lack of correlation in the input from the two eyes. However, if the eyes are assumed to be aligned during a recovery period after MD, the properties of the noise $n_j(t)$ become important. As the variance of the noise increases (i.e. as $\overline{n^2}$ goes up), the rate of recovery of the initially deprived eye synapses increases. Since $\overline{n^2}$ is always assumed to be nonzero, using Eq. 17 for the input to the cell always leads to a stable, selective equilibrium state that is binocular.

DISCUSSION

1. Comparison with experiment

Our simulations show that the BCM theory leads to an evolution of the cell response to equilibrium states in agreement with "classical" visual deprivation experiments in kitten striate cortex. The simulations were produced with a single set of parameter settings and each simulation was started using the equilibrium state of a preceding simulation (with the exception of NR which started from randomized synaptic weights). Starting a simulation from the equilibrium state of a preceding simulation is not necessary; however, this facilitates comparison of simulations with experimental results.

Of particular interest is the relative timing for various effects during the simulated forms of deprivation (Figure 14). To facilitate comparisons of the timing of synaptic modification across the various simulations, as well as comparisons of simulations with actual experimental observations, we can convert simulation time (i.e. iteration) to real time. It is understood, of course, that this conversion is primarily for comparative purposes, and would be affected by such things as the age of the animal, periods of sleep, etc. These caveats notwithstanding, we can use MD to calculate a conversion of iteration to real time. At the height of the critical period MD leads to a loss of responsiveness to the closed eye in approximately 24 hours (Mioche and Singer, 1989). In the simulation, with our parameter choice, the closed eye disconnects in approximately 67,000 iterations. Therefore, with these parameters, 1 iteration corresponds to about 1.3 seconds of real time.

Thus, in the simulation of RS, the deprived eye disconnects significantly in 24 hours and almost completely by the 48th hour. During the BD simulation, there is a significant loss in responsiveness during the first 24 hours; however, thereafter some responsiveness is retained. ST simulations lead to a disconnection of one eye in approximately 14 hours, which is more severe than MD. During NR simulations, once the cell response begins to increase after about 10 hours of patterned experience, it climbs rapidly during the next 14 hours to near its final state. The recovery of the previously closed eye during RS simulations also occurs on the order of a day. Notice in the RS simulation, however, that

the previously closed eye does not begin to recover until θ is sufficiently low to allow the poor cell response to exceed it; this takes about 24 hours. By this time the currently closed eye is almost completely disconnected. When normal, binocular input is restored after a period of MD, the recovery of the closed eye in the simulation takes place on a much longer timescale, showing gradual gains over 3 days.

The kinetics of our simulations are in good agreement with experimental results. The loss of closed eye responsiveness during simulations of MD and RS occurs over approximately the same timescales of 24 hours and 24 to 48 hours, respectively, agreeing with the experimental findings of Mioche and Singer (1989). Mioche and Singer (1989) hypothesize that the same mechanism is at play in the disconnection of the closed eye during these two experiments; this idea can be accounted for in the BCM theory by the theoretical result that noise input to a set of synapses at a time when the modification threshold is high leads to a decrement in their respective synaptic weights. The rapid loss of one eye's synaptic efficacy during the ST simulation is actually more severe than the deterioration of the closed eye synaptic weights during MD. (This is one illustration of a general consequence of the theory - the rate of disconnection increases with increased fluctuations of input to the deteriorating eye.) Although we know of no experimental evidence that specifies the absolute rate at which one eye's responsiveness is lost during ST, the final monocular state of $m(t)$ obtained during the ST simulation agrees with all of the experimental findings. The loss of responsiveness during the BD simulation also has many features in agreement with experiment: it is less severe than MD on the short-term and leads to a generally poor, unselective response on the long-term.

The evolution of open eye synaptic weights during the simulation of MD and the effective eye synaptic weights during the simulation of ST leads to an enhancement of the cell response to that eye. In the case of the MD simulation the enhancement in the open eye response does not occur until after the closed eye is almost completely disconnected, which appears to be in keeping with the experimental results of Mioche and Singer (1989) in those instances where they do see an enhancement of the open eye response. Experimental confirmation of the increase in effective eye response during the

ST simulation is more difficult to determine since there are apparently no studies that have directly investigated this point. However, we emphasize that, unlike the disconnection of the closed eye during MD and RS, this increased responsiveness depends on parameters, the form of θ and the properties of the equilibrium state obtained during the prior period of NR.

The largest potential discrepancy between the kinetics of the simulations and experimental findings is the quick recovery of the currently open eye during RS. Experimentally, the recovery of this eye is a slow and incomplete process, taking from 48 to 72 hours just to exhibit partial recovery (Mioche and Singer, 1989). In the simulation, on the other hand, the recovery is rapid and complete within approximately 24 hours; once the cell response to patterned input begins to exceed θ the synapses receiving the patterned input recover in a robust fashion. To slow down the recovery of the open eye during RS other features would likely have to be incorporated; these might include changes in modifiability with increasing age (i.e. the critical period) and the potential irreversible loss of some connections that are deprived for too long. It is also possible that Mioche and Singer (1989) underestimate the speed of recovery of a healthy cell since they are recording from neurons that may have deteriorated after several days of chronic recording.

2. Sensitivity of results to parameter values

We now discuss the dependence of our results on the choice of parameters (see Table 3). Consider first RS. As mentioned, Mioche and Singer (1989) find that the newly closed eye's ability to drive the postsynaptic cell significantly lessens before the currently open eye input to the cell strengthens. In order for us to obtain this result the modification threshold θ must drop sufficiently slowly with the advent of the RS while $\overline{n^2} \neq 0$ along the closed eye fibers (Eq. 23a). Keeping θ high guarantees both the disconnection of the closed eye from the cell, as long as $\overline{n^2} \neq 0$, and the lack of a recovery in the open eye until the closed eye disconnects. Comparisons with experiment indicate that θ should drop from its pre-RS level to the low level of the postsynaptic response during the initial stages of a RS in approximately 24 to 48 hours.

The rate of change of θ is determined by the memory of the cell response time average (τ) and the definition of θ . In these simulations τ corresponds to 22 minutes of real time. As we have discussed before, τ cannot be arbitrarily increased (for a given value of η) without introducing unwanted oscillations. Setting τ approximately equal to 24 hours would produce the desired evolution of the synapses during RS; however, τ would now be much too large for the current value of η to lead to acceptable behavior during NR (Section 1, Results). Therefore, for θ to stay above the prevailing low postsynaptic response (c) for more than 22 minutes during the initial stages of a RS, it must have a dependence on something other than just the response c itself. In this paper we have defined θ in terms of $c_a(t)$ and, as the results indicate, this form of θ produces the desired evolution of the synapses during RS.

The critical difference between $c(t)$ and $c_a(t)$ in the time average for θ is the average level of the spontaneous activity (d_s). As d_s increases, $c_a(t)$ depends less upon the cell response to patterned input per se and more upon the overall average fiber activity, including the spontaneous activity, as well as on the synaptic weights themselves. Making θ dependent on total depolarization rather than deviations of the depolarization from its average level reduces its sensitivity to sudden changes in the visual environment. When removal of patterned input to a cell leads to a radical change in the cell response, θ adjusts more slowly to the change with larger values of d_s . In the current simulations $d_s = 5.0$ which keeps θ sufficiently high to prevent the open eye from recovering during RS until the closed eye is almost completely disconnected.

With our parameter choice, the maximum displacement from spontaneous LGN fiber activity for pattern input is 1.0 ($d_{\text{peak}} + d_{\text{base}} - d_s = 1.0$), which is much smaller than d_s (Table 2). However, it is not required that the average level of the spontaneous activity be as large as 80% of the total LGN response to patterned input to produce a significant disconnection of the closed eye during RS before the open eye recovers. There are two reasons. First, for d_s as small as 0.2 (20% of the LGN response to patterns), there is a significant ($\approx 60\%$) drop in the closed eye response before the open eye recovers. Second, the magnitude of d_s can also be interpreted as the frequency of occurrence of

patterned LGN input activity against a continuous background of noise. From this point of view increasing d_s amounts to decreasing the occurrence of patterned LGN input as compared to noisy LGN input. Simulations with $d_{\text{peak}} = 100$, $d_s = 10$ and patterned input occurring every 6th iteration between 5 consecutive iterations of noise input leads to an evolution of the synaptic weights that is quite similar to Figures 6-13.

For $\overline{n^2} \neq 0$ the closed eye is guaranteed to disconnect during MD since the open eye ratio of optimal to nonoptimal patterns remains small (Eq. 24). Therefore, for the simulations to be consistent with the MD experimental findings $\overline{n^2} \neq 0$. Notice that the mechanism of the closed eye disconnection is the same during MD and RS, as long as θ drops slowly during RS and the cell response to open eye input remains selective during MD.

Two other experiments that help set the magnitude of $\overline{n^2}$ are ST and RE. In the ST simulation one of the two eyes completely disconnects from the cell in approximately 14 hours, whereas it takes approximately 24 hours for a disconnection of the closed eye input during MD. If the rates of change of the two sets of synapses actually occur on the same timescale during ST and MD, then the time for disconnection in MD could be decreased to 14 hours by increasing the magnitude of $\overline{n^2}$. However, changing $\overline{n^2}$ also changes the rate at which the closed eye recovers during RE (Section 6, Results). Therefore, detailed quantitative knowledge of the time rates of cell response changes during experiments of MD, ST and RE would lead to more stringent constraints on $\overline{n^2}$.

With η , τ and $\overline{n^2}$ set by NR, MD, RS, ST and RE, and with a given form of θ , the evolution of the synapses during the initial stages of BD is fixed. With the onset of BD the cell response drops rapidly. In the current simulations both eye's LGN-cortical synaptic weights significantly weaken as θ drops to the prevailing postsynaptic cell response over the first 24 to 48 hours. The situation is reminiscent of RS where the cell response is low and θ is initially high and drops slowly due to the large value of d_s ; however, in the BD simulation there is no patterned input to an eye that eventually increases cell response, and therefore θ . It follows that once θ reaches the low response level during BD, the rate of weakening of the synaptic weights gradually diminishes.

As detailed in the **Results**, the long-term evolution of the synapses during BD depends on parameters such as \bar{n} and $\overline{c_{\text{noise}}^2}$, in addition to $\overline{n^2}$. The parameters \bar{n} and $\overline{c_{\text{noise}}^2}$ have subtle effects on the evolution of the synapses during simulations of NR, MD, RS, and ST, as well. For example, with the onset of patterned binocular input to “immature” synapses (i.e. NR), the high level of $\overline{c_{\text{noise}}^2}$ prevents both eyes from immediately acquiring selectivity and responsiveness (Figure 14); with the current parameter settings it takes about 10 hours for the cell to sort out the LGN evoked response from the high levels of postsynaptic noise. The eventual acquisition of selectivity in the presence of such large levels of noise ($\overline{c_{\text{noise}}^2} = 33.3$, Table 2) demonstrates that the system is robust to large fluctuations in the postsynaptic response. In the ST simulation the slight retention of response to stimulation of the disconnected eye is also due to the large level of $\overline{c_{\text{noise}}^2}$; if $\overline{c_{\text{noise}}^2}$ is set to 0, then the weak eye immediately loses its ability to evoke any response from the cell. Finally, large levels of $\overline{c_{\text{noise}}^2}$ generally decrease the rate at which the closed eye synapses disconnect during MD and RS since the assumptions leading to Eq. 23a are weakened.

Apart from BD, other effects of changing \bar{n} appear during MD and RS. As \bar{n} departs from 0, the approximations leading to Eq. 23a become less valid (see appendix). Therefore, the rate of disconnection of the closed eye synapses begins to decrease for \bar{n} sufficiently large in both the MD and RS cases.

The parameters p and c_0 are not rigidly set by simulations of the “classical” experiments. In the current simulations we choose $p = 2$; this produces a nonlinearity in the calculation of θ that is in keeping with the theory. c_0 is chosen sufficiently large to insure that θ is below the majority of the cell’s responses at the start of NR, leading to an initial enhancement of the cell’s responsiveness. Other than these considerations, there are as yet no binding experimental constraints on p and c_0 .

The slopes of ϕ at the origin (ϵ_0) and at θ (ϵ_θ) are strictly constrained, such that $\epsilon_0 < 0$ and $\epsilon_\theta > 0$. As Eq. 23 indicates, their magnitudes provide another degree of freedom in controlling the disconnection of the closed eye, or eyes, during MD, RS and BD. However, there are not yet any experimental results that directly determine these

magnitudes. The uncertainty in the magnitudes ϵ_0 and ϵ_θ suggests a certain freedom in specifying the exact functional form of ϕ . Although $\phi < 0$ for $0 < c < \theta$ and $\phi > 0$ for $c > \theta$, as many simulations show, the exact form of ϕ in these two regions does not appear to be critical. Perhaps of more interest is the dependence of ϕ on c for $c < 0$. The only theoretical constraint on ϕ is that it must not be too negative for $c < 0$ (see appendix).

In summary, NR places constraints on p , τ , η and c_0 . RS, with the closed eye disconnecting before the open eye recovers, places constraints on τ and the form of θ . Once τ and the form of θ are set by RS, the evolution of the synaptic weights during BD is fixed. The closed eye disconnection during MD, RS and BD indicates that $\overline{n^2} > 0$. The rate of disconnection of the closed eye during MD and RS as compared to the loss of cell response to one eye's input during ST, together with the recovery of the previously closed eye during RE, places constraints on the magnitude of $\overline{n^2}$. The parameter settings \overline{n} and $\overline{c_{noise}^2}$ have secondary consequences that affect the equilibrium states and the rapidity with which they are reached during simulations of several of the paradigms, especially BD. In this paper we have set the non-LGN postsynaptic fluctuations about the cell's spontaneous level, so that $\overline{c_{noise}}$ is 0. With the constraints on the parameters just outlined, a major implication of this investigation is that the modification threshold θ changes from its value acquired during monocular deprivation to near 0 on the order of 24 to 48 hours of reverse suture.

3. Alternate forms for θ

We emphasize that the definition of θ in Eq. 16 is just one of several possibilities that has the properties outlined in the Methods (Section 3). Another possibility, for example, is θ defined by Eq. 15, where the nonlinearity is applied to the cell response before the averaging takes place. Although the different dependences of θ have relatively small effects on the evolution of synapses during the different paradigms described in the present work, they have very different mathematical properties and strikingly different physiological implications. Preliminary investigation indicates that they might also have different consequences on the simulated outcomes of various pharmacological exper-

iments, such as the blockade of cortical NMDA receptors (Bear et al., 1990). Regardless of its exact form, the RS finding of Mioche and Singer (1989) implies that the threshold slides from its NR value to near 0 in approximately 24 to 48 hours.

4. Extension to networks

The single cell results presented here can be interpreted within the framework of a cortical network of cells. As mentioned in the introductory paragraphs of the Methods, placing the single cell in a mean-field network does not change the position and/or stability properties of the equilibrium states; however, there may be changes in the dynamics of the evolution of the synapses during simulations of the paradigms considered here that may refine some of the constraints on the parameters. In this context the validity of the mean-field approximation becomes an interesting experimental question. For if the intracortical connections can be described as an average effect on a cell, then the single cell simulations are an accurate description of what is happening in a network.

Placing the single cell in a network of cells has other important consequences. For example, in the single cell simulations the spontaneous activity increases and decreases with the cell's synaptic weights (Eq. 9). However, in a network of cells the spontaneous activity of any one cell is not necessarily tied so closely to its LGN input. In fact, all of the influence to a cell from other excitatory and inhibitory cells in a network could possibly make the spontaneous activity of a cell to some extent independent of its LGN input. This is a complicating factor not explicitly considered in the present work.

5. Possible mechanisms

We are now led to the question of the biological basis of the theoretical form of modification employed successfully in this paper. Our work suggests that the modifications of interest may occur mainly at excitatory geniculocortical synapses; the postsynaptic responses at these synapses are mediated by excitatory amino acid receptors. Thus, mechanisms linked to excitatory amino acid receptors seem to be an appropriate place to look for the molecular basis of visual cortical plasticity.

Theory requires that input activity that coincides with postsynaptic activation beyond θ leads to an enhancement of synaptic efficacy. Work on the hippocampus and

visual cortex *in vitro* has shown that the pairing of input activity with postsynaptic depolarization can lead to a long-term potentiation (LTP) of the active synapses (Kelso et al., 1986; Gustaffson et al., 1987; Artola et al., 1990; Frégnac et al., 1990). In these locations LTP induction appears to depend upon a voltage-dependent Ca^{2+} conductance that is mediated by N-methyl-D-aspartate (NMDA) receptors. Thus, Bear et al. (1987) have proposed that θ might be related to the membrane potential at which the NMDA receptor dependent Ca^{2+} flux reaches the threshold for inducing synaptic long-term potentiation.

One consequence of the association of θ with NMDA receptor mechanisms is that input activity which consistently fails to correlate with postsynaptic activation sufficient to recruit an NMDA receptor mediated Ca^{2+} flux should lead to a long-term depression (LTD) of synaptic efficacy. Such a form of modification has been observed recently in both hippocampus (Chattarji et al., 1989; Stanton and Sejnowski, 1989; Staubli and Lynch, 1990) and visual cortex (Artola and Singer, 1990; Bear et al., 1990; Frégnac et al., 1990; Kimura et al., 1990). The mechanism of this form of plasticity is unknown; however, recent experimental evidence suggests that activation of a class of non-NMDA receptors (the "metabotropic" quisqualate receptors) stimulates the hydrolysis of membrane inositol phospholipids in kitten striate cortex (Dudek and Bear, 1989). These considerations have led to the suggestion that phosphoinositide hydrolysis might provide the biochemical trigger for use-dependent decreases in synaptic efficacy (Bear, 1988; Dudek and Bear, 1989; Bear and Cooper, 1990). In this context it is interesting to note that the developmental time-course of excitatory amino acid stimulated phosphoinositide turnover correlates precisely with the critical period for synaptic modification in kitten visual cortex (Dudek and Bear, 1989).

Another consequence of the association of θ with NMDA receptor mechanisms is that the effectiveness of NMDA receptor activation in triggering synaptic modification should be a function of the recent history of cortical cell activity (Bear et al., 1987; Bear and Cooper, 1990). In principle, this could occur in a number of ways including the activity-dependent regulation of NMDA receptor sensitivity, postsynaptic Ca^{2+} buffers

or pumps, Ca^{2+} activated enzymes, opposing mechanisms of synaptic weakening, etc.

Our work suggests that the value of θ is low after approximately 48 hours of binocular deprivation in kitten striate cortex. Recent data suggests that although the density of NMDA receptors is unaffected by 4-6 days of binocular deprivation (Reynolds and Bear, 1990), NMDA stimulated $^{45}\text{Ca}^{2+}$ accumulation is significantly decreased in visual cortical slices prepared from binocularly deprived (but not monocularly deprived) animals (Feldman et al., 1990). One explanation (among many) for this result is that cortical inactivity causes a decrease in intracellular Ca^{2+} -binding proteins. This hypothesis is particularly attractive in light of work by Holmes and Levy (1990) and Zador et al. (1990) suggesting that induction of LTP by NMDA receptor activation might be particularly sensitive to changes in calcium buffers in dendritic spines. Regardless of the mechanism, however, these $^{45}\text{Ca}^{2+}$ uptake experiments indicate that cortical calcium homeostasis can vary significantly as a function of activity.

Detailed discussions of these hypothetical molecular mechanisms have been published elsewhere (e.g. Bear and Cooper, 1990; Bear and Dudek, 1990). Regardless of whether these specific hypotheses ultimately prove to be correct, this work demonstrates that the theory developed here can serve as a bridge between molecular mechanisms and a description of visual cortical plasticity. We are able to follow a long chain of arguments and to connect in a fairly precise way, various hypotheses with their consequences. The understanding this provides, we believe, makes visual cortex an ideal preparation with which to study the mechanisms of experience-dependent synaptic modification and its relation to behavior.

Acknowledgements:

This work was supported in part by the Office of Naval Research (Contract #N00014-86-K-0041), the National Science Foundation (Contract #'s EET-8719102 and DIR-8720084) and the Army Research Office (Contract #DAAL03-88-K-0116). We wish to thank Joshua I. Gold and Daniel G. Aliaga for their invaluable assistance in constructing the color figures used in this paper.

REFERENCES

- Albus K, Wolf W (1984) Early post-natal development of neuronal function in the kitten's visual cortex: a laminar analysis. *J. Physiol.* 348:153-185.
- Artola A, Bröcher S, Singer W (1990) Different voltage-dependent thresholds for inducing long-term depression and long-term potentiation in slices of rat visual cortex. *Nature* 347:69-72.
- Artola A, Singer W (1990) The involvement of N-methyl-D-aspartate receptors in induction and maintenance of long-term potentiation in rat visual cortex. *Eur. J. Neurosci.* 2:254-269.
- Barlow HB (1975) Visual experience and cortical development. *Nature* 258:199-204.
- Barlow HB, Levick WR (1969) Changes in the maintained discharge with adaptation level in the cat retina. *J. Physiol.* 202:699-718.
- Barlow HB, Pettigrew JD (1971) Lack of specificity of neurones in the visual cortex of young kittens. *J. Physiol.* 218:98P-100P.
- Bear MF (1988) Involvement of excitatory amino acid receptors in the experience-dependent development of visual cortex. In: *Frontiers in excitatory amino acid research* (Cavalheiro E, Lehmann J and Turski L, eds), Vol. 46, pp 393-401. New York: Alan R. Liss, Inc.
- Bear MF, Cooper LN, Ebner FF (1987) A physiological basis for a theory of synapse modification. *Science* 237:42-48.
- Bear MF, Cooper LN (1990) Molecular mechanisms for synaptic modification in the visual cortex: interaction between theory and experiment. In: *Neuroscience and connectionist theory* (Gluck MA and Rumelhart DE, eds), pp 65-93. Hillsdale, New Jersey: Lawrence Erlbaum Associates.
- Bear MF, Dudek SM (1990) Excitatory amino acid stimulated phosphoinositide turnover:

pharmacology, development and role in visual cortical plasticity. *Ann. NY Acad. Sci.*, in press.

Bear MF, Kleinschmidt A, Gu Q, Singer W (1990) Disruption of experience-dependent synaptic modifications in striate cortex by infusion of an NMDA receptor antagonist. *J. Neurosci.* 10(3):909-925.

Bienenstock EL, Cooper LN, Munro PW (1982) Theory for the development of neuron selectivity: Orientation specificity and binocular interaction in visual cortex. *J. Neurosci.* 2:32-48.

Blakemore C (1976) The conditions required for the maintenance of binocularity in the kitten's visual cortex. *J. Physiol.* 261:423-444.

Blakemore C, Van Sluyters RC (1974a) Experimental analysis of amblyopia and strabismus. *Brit. J. Ophthalmol.* 58:176-182.

Blakemore C, Van Sluyters RC (1974b) Reversal of the physiological effects of monocular deprivation in kittens: Further evidence for a sensitive period. *J. Physiol.* 237:195-216.

Blakemore C, Van Sluyters RC (1975) Innate and environmental factors in the development of the kitten's visual cortex. *J. Physiol.* 248:663-716.

Blakemore C, Eggers HM (1978) Effects of artificial anisometropia and strabismus on the kitten's visual cortex. *Arch. ital. Biol.* 116:385-389.

Blasdel GG, Pettigrew JD (1978) Effect of prior visual experience on cortical recovery from the effects of unilateral eyelid suture in kittens. *J. Physiol.* 274:601-619.

Blasdel GG, Pettigrew JD (1979) Degree of interocular synchrony required for maintenance of binocularity in kitten's visual cortex. *J. Neurophysiol.* 42:1692-1710.

Bonds AB (1979) Development of orientation tuning in the visual cortex of kittens. In: *Developmental Neurobiology of Vision* (Freeman RD, ed), pp 31-41. New York: Plenum.

Braastad BO, Heggelund P (1985) Development of spatial receptive-field organization

and orientation selectivity in kitten striate cortex. *J. Neurophysiol.* 53:1158-1178.

Buisseret P, Imbert M (1976) Visual cortical cells: Their developmental properties in normal and dark reared kittens. *J. Physiol.* 255:511-525.

Buisseret P, Gary-Bobo E, Imbert M (1978) Ocular motility and recovery of orientational properties of visual cortical neurones in dark-reared kittens. *Nature* 272:816-817.

Buisseret P, Gary-Bobo E, Imbert M (1982) Plasticity in the kitten's visual cortex: Effects of the suppression of visual experience upon the orientational properties of visual cortical cells. *Dev. Brain Res.* 4:417-426.

Burchfiel JL, Duffy FH (1981) Role of intracortical inhibition in deprivation amblyopia: Reversal by microiontophoretic bicuculline. *Brain Res.* 206:479-484.

Chattarji S, Stanton PK, Sejnowski TJ (1989) Commissural synapses, but not mossy fiber synapses, in hippocampal field CA3 exhibit associative long-term potentiation and depression. *Brain Res.* 495:145-150.

Cooper LN, Liberman F, Oja E (1979) A theory for the acquisition and loss of neuron specificity in visual cortex. *Biol. Cybernet.* 33:9-28.

Cooper LN, Scofield CL (1988) Mean-field theory of a neural network. *Proc. Natl. Acad. Sci. USA* 85:1973-1977.

Cynader M (1983) Prolonged sensitivity to monocular deprivation in dark-reared cats: Effects of age and visual exposure. *Dev. Brain Res.* 8:155-164.

Cynader M, Berman N, Hein A (1976) Recovery of function in cat visual cortex following prolonged deprivation. *Exp. Brain Res.* 25:139-156.

Cyander M, Mitchell DE (1977) Monocular astigmatism effects on kitten visual cortex development. *Nature* 270:177-178.

Dudek SM, Bear MF (1989) A biochemical correlate of the critical period for synaptic modification in the visual cortex. *Science* 246:673-675.

Duffy FH, Snodgrass SR, Burchfiel JL, Conway JL (1976) Bicuculline reversal of deprivation amblyopia in the cat. *Nature* 260:256-257.

Feldman D, Sherin JE, Press WA, Bear MF (1990) N-methyl-D-aspartate-evoked calcium uptake by kitten visual cortex maintained *in vitro*. *Exp. Brain Res.* 80:252-259.

Freeman RD, Mallach R, Hartley S (1981) Responsivity of normal kitten striate cortex deteriorates after brief binocular deprivation. *J. Neurophysiol.* 45:1074-1084.

Freeman RD, Olson C (1982) Brief periods of monocular deprivation in kittens: Effects of delay prior to physiological study. *J. Neurophysiol.* 47:139-150.

Freeman RD, Ohzawa I (1988) Monocularly deprived cats: Binocular tests of cortical cells reveal functional connections from the deprived eye. *J. Neurosci.* 8(2):2491-2506.

Frégnac Y, Imbert M (1978) Early development of visual cortical cells in normal and dark-reared kittens: Relationship between orientation selectivity and ocular dominance. *J. Physiol.* 278:27-44.

Frégnac Y, Imbert M (1984) Development of neuronal selectivity in primary visual cortex of cat. *Physiol. Rev.* 64:325-434.

Frégnac Y, Smith D, Friedlander MJ (1990) Postsynaptic membrane potential regulates synaptic potentiation and depression in visual cortical neurons. *Soc. Neurosci. Abst.* 16:331.10.

Greuel JM, Luhmann HJ, Singer W (1987) Evidence for a threshold in experience-dependent long-term changes of kitten visual cortex. *Dev. Brain Res.* 34:141-149.

Gustafsson B, Wigström H, Abraham WC, Huang YY (1987) Long-term potentiation in the hippocampus using depolarizing current pulses as the conditioning stimulus to single volley synaptic potentials. *J. Neurosci.* 7:774-780.

Holmes WR, Levy WB (1990) Insights into associative long-term potentiation from computational models of NMDA receptor-mediated calcium influx and intracellular calcium

concentration changes. *J. Neurophysiol.* 63:1148-1168.

Hubel DH, Wiesel TN (1961) Integrative action in the cat's lateral geniculate body. *J. Physiol.* 155:385-398.

Hubel DH, Wiesel TN (1962) Receptive fields, binocular interaction and functional architecture in the cat's visual cortex. *J. Physiol.* 160:106-154.

Hubel DH, Wiesel TN (1963) Receptive fields of cells in striate cortex of very young, visually inexperienced kittens. *J. Neurophysiol.* 26:994-1002.

Hubel DH, Wiesel TN (1965) Binocular interaction in striate cortex of kittens reared with artificial squint. *J. Neurophysiol.* 28:1041-1059.

Hubel DH, Wiesel TN (1970) The period of susceptibility to the physiological effects of unilateral eye closure in kittens. *J. Physiol.* 206:419-436.

Ikeda H, Tremain KE (1977) Different causes for amblyopia and loss of binocularity in squinting kittens. *J. Physiol.* 269:26-27P.

Imbert M, Buisseret P (1975) Receptive field characteristics and plastic properties of visual cortical cells in kittens reared with or without visual experience. *Exp. Brain Res.* 22:25-36.

Intrator N (1990) A neural network for feature extraction. In: *Advances in Neural Information Processing Systems 2* (Touretzky DS, ed), pp 719-726. San Mateo, California: Morgan Kaufmann.

Kelso SR, Ganong AH, Brown TH (1986) Hebbian synapses in hippocampus. *Proc. Natl. Acad. Sci. USA* 83:5326-5330.

Kimura F, Tsumoto T, Nishigori A, Yoshimura Y (1990) Long-term depression but not potentiation is induced in Ca^{2+} -chelated visual cortex neurons. *NeuroReport*, in press.

Kratz KE, Spear PD (1976) Effects of visual deprivation and alterations in binocular competition on responses of striate cortex neurons in the cat. *J. Comp. Neur.* 170:141-

151.

Kratz KE, Spear PD, Smith DC (1976) Postcritical- period reversal of effects of monocular deprivation on striate cortex cells in the cat. *J. Neurophysiol.* 39:501-511.

Kuffler SW, Fitzhugh R, Barlow HB (1957) Maintained activity in the cat's retina in light and darkness. *J. Gen. Physiol.* 40:683-702.

Linsker R (1986) From basic network principles to neural architecture. *Proc. Natl. Acad. Sci. USA* 83:7508-7512, 8390-8394, 8779-8783.

Malsburg, Ch. von der (1973) Self-organization of orientation sensitive cells in the striate cortex. *Kybernetik* 14: 85-100.

Mastrorarde DN (1983a) Correlated firing of cat retinal ganglion cells. I. Spontaneously active inputs to X- and Y-cells. *J. Neurophysiol.* 49:303-324.

Mastrorarde DN (1983b) Correlated firing of cat retinal ganglion cells. II. Responses of X- and Y-cells to single quantal events. *J. Neurophysiol.* 49:325-349.

Mastrorarde DN (1989) Correlated firing of cat retinal ganglion cells. *TINS* 12:75-80.

Miller KD, Keller JB, Stryker MP (1989) Ocular dominance column development: Analysis and simulation. *Science* 245:605-615.

Mioche L, Singer W (1988) Long-term recordings and receptive field measurements from single units of the visual cortex of awake unrestrained kittens. *J. Neurosci. Methods* 26:83-94.

Mioche L, Singer W (1989) Chronic recordings from single sites of kitten striate cortex during experience-dependent modifications of receptive-field properties. *J. Neurophysiol.* 62:185-197.

Mitchell DE, Cyander M, Movshon JA (1978) Recovery from the effects of monocular deprivation in kittens. *J. Comp. Neur.* 176:53-64.

Movshon JA (1976) Reversal of the physiological effects of monocular deprivation in the

kitten's visual cortex. *J. Physiol.* 261:125-174.

Movshon JA, Dürsteler MR (1977) Effects of brief periods of unilateral eye closure on the kitten's visual system. *J. Neurophysiol.* 40:1255-1265..

Movshon JA, Van Sluyters RC (1981) Visual neural development. *Ann. Rev. Psychol.* 32:477-522.

Mower GD, Berry D, Burchfiel JL, Duffy FH (1981) Comparison of the effects of dark rearing and binocular suture on development and plasticity of cat visual cortex. *Brain Res.* 220:255-267.

Nass MM, Cooper LN (1975) A theory for the development of feature detecting cells in visual cortex. *Biol. Cybernet.* 19:1-18.

Ohzawa I, Freeman RD (1986a) The binocular organization of simple cells in the cat's visual cortex. *J. Neurophysiol.* 56:221-242.

Ohzawa I, Freeman RD (1986b) The binocular organization of complex cells in the cat's visual cortex. *J. Neurophysiol.* 56:243-259.

Olson CR, Freeman RD (1975) Progressive changes in kitten striate cortex during monocular vision. *J. Neurophysiol.* 38:26-32.

Olson CR, Freeman RD (1978) Monocular deprivation and recovery during sensitive period in kittens. *J. Neurophysiol.* 41:65-74.

Pérez R, Glass L, Shlaer R (1975) Development of specificity in the cat visual cortex. *J. Math. Biol.* 1:275-288.

Pettigrew JD (1974) The effect of visual experience on the development of stimulus specificity by kitten cortical neurones. *J. Physiol.* 237:49-74.

Reiter HO, Stryker MP (1988) Neural plasticity without action potentials: Less active inputs become dominant when kitten visual cortical cells are pharmacologically inhibited. *Proc. Natl. Acad. Sci. USA* 85:3623-3627.

- Reynolds IJ, Bear MF (1990) The effects of age and visual experience on [³H]MK801 binding to NMDA receptors in the kitten visual cortex. *Exp. Brain Res.*, submitted.
- Saul AB, Clothiaux EE (1986) Modeling and simulation III: Simulation of a model for development of visual cortical specificity. *J. Electrophysiol. Tech.* 13:279-306.
- Scofield CL, Cooper LN (1985) Development and properties of neural networks. *Contemp. Phys.* 26:125-145.
- Sillito AM, Kemp JA, Blakemore C (1981) The role of GABAergic inhibition in the cortical effects of monocular deprivation. *Nature* 291:318-320.
- Singer W (1977) Effects of monocular deprivation on excitatory and inhibitory pathways in cat striate cortex. *Exp. Brain Res.* 30:25-41.
- Stanton PK, Sejnowski TJ (1989) Associative long-term depression in the hippocampus induced by hebbian covariance. *Nature* 339:215-218.
- Staubli U, Lynch G (1990) Stable depression of potentiated synaptic responses in the hippocampus with 1-5 Hz stimulation. *Brain Res.* 513:113-118.
- Tsumoto T, Suda K (1978) Evidence for excitatory connections from the deprived eye to the visual cortex in monocularly deprived kittens. *Brain Res.* 153:150-156.
- Van Sluyters RC, Levitt FB (1980) Experimental strabismus in the kitten. *J. Neurophysiol.* 43:686-699.
- Watkins DW, Wilson JR, Sherman SM (1978) Receptive-field properties of neurons in binocular and monocular segments of striate cortex in cats raised with binocular lid suture. *J. Neurophysiol.* 41:322-337.
- Wiesel TN, Hubel DH (1963) Single-cell responses in striate cortex of kittens deprived of vision in one eye. *J. Neurophysiol.* 26:1003-1017.
- Wiesel TN, Hubel DH (1965) Comparison of the effects of unilateral and bilateral eye closure on cortical unit responses in kittens. *J. Neurophysiol.* 28:1029-1040.

Yinon U (1976) Age dependence of the effect of squint on cells in kittens' visual cortex. *Exp. Brain Res.* 26:151-157.

Yinon U, Auerbach E, Blank M, Friesenhausen J (1975) The ocular dominance of cortical neurons in cats developed with divergent and convergent squint. *Vision Res.* 15:1251-1256.

Zador A, Koch C, Brown TH (1990) Biophysical model of a Hebbian synapse. *Proc. Natl. Acad. Sci. USA* 87:6718-6722.

APPENDIX

To show why the closed eye disconnects during MD we analyze in more detail the original arguments given by BCM (1982). According to Eq. 13 the modification of the synaptic weights occurs as the product of the input activity d_j and ϕ . When nonoptimal patterns are presented to the open (right) eye and noise to the deprived (left) eye, the cell response falls near zero. At this low level of cell response, ϕ can be approximated by a line with a negative slope $-\epsilon$; that is, $\phi \approx -\epsilon c$ (Figure 8). Therefore, the j^{th} left eye synaptic weight modifies as the product of $-\epsilon c$ and its input activity $n_j^l(t)$:

$$\frac{dm_j^l(t)}{dt} \approx \eta(-\epsilon c) n_j^l(t). \quad (A1)$$

Substituting the definition of c (Eq. 12) into Eq. A1 gives

$$\frac{dm_j^l(t)}{dt} \approx \eta(-\epsilon) \left[\mathbf{m}^l(t) \cdot \mathbf{n}^l(t) n_j^l(t) + \mathbf{m}^r(t) \cdot \mathbf{d}^r(t) n_j^l(t) \right] \quad (A2a)$$

or

$$\frac{dm_j^l(t)}{dt} \approx \eta(-\epsilon) \left[\left(\sum_{k=1}^{N_{gl}} m_k^l(t) n_k^l(t) \right) n_j^l(t) + \left(\sum_{k=1}^{N_{gr}} m_k^r(t) d_k^r(t) \right) n_j^l(t) \right]. \quad (A2b)$$

Averaging Eq. A2b over N_0 nonoptimal open eye patterns, where N_0 is small compared to the number of iterations necessary for a significant change in the synaptic weights, yields

$$\overline{\overline{\frac{dm_j^l(t)}{dt}}} \approx \eta(-\epsilon) \left[\sum_{k=1}^{N_{gl}} m_k^l(t) \left(\frac{1}{N_0} \sum_{s=1}^{N_0} n_k^l(t_s) n_j^l(t_s) \right) + \sum_{k=1}^{N_{gr}} m_k^r(t) \left(\frac{1}{N_0} \sum_{s=1}^{N_0} d_k^r(t_s) n_j^l(t_s) \right) \right], \quad (A3)$$

where the double bar represents the average change to the j^{th} left eye synaptic weight over the N_0 nonoptimal patterns. Note that t_s , $s = 1, \dots, N_0$, denotes N_0 iterations of the simulation centered at time t ; the synaptic weights are assumed to change negligibly during the N_0 iterations. Since the noise inputs to the different left eye fibers are independent of each other,

$$\frac{1}{N_0} \sum_{s=1}^{N_0} n_k^l(t_s) n_j^l(t_s) = \left[\frac{1}{N_0} \sum_{s=1}^{N_0} n_k^l(t_s) \right] \left[\frac{1}{N_0} \sum_{s=1}^{N_0} n_j^l(t_s) \right] = (\bar{n})^2 \quad (A4a)$$

for $k \neq j$ and

$$\frac{1}{N_0} \sum_{s=1}^{N_0} n_k^l(t_s) n_j^l(t_s) = \frac{1}{N_0} \sum_{s=1}^{N_0} n_j^l(t_s)^2 = \overline{n^2} \quad (A4b)$$

for $k = j$. Using Eq. 8 for $d_k^l(t_s)$,

$$\frac{1}{N_0} \sum_{s=1}^{N_0} d_k^l(t_s) n_j^l(t_s) = \frac{1}{N_0} \sum_{s=1}^{N_0} d_k^{\omega,r}(t_s) n_j^l(t_s) + \frac{1}{N_0} \sum_{s=1}^{N_0} n_k^l(t_s) n_j^l(t_s). \quad (A5a)$$

Since the noise on the right eye fibers is independent of the noise and patterns on the left eye fibers, Eq. A5a is equivalent to

$$\left[\frac{1}{N_0} \sum_{s=1}^{N_0} d_k^{\omega,r}(t_s) \right] \left[\frac{1}{N_0} \sum_{s=1}^{N_0} n_j^l(t_s) \right] + \left[\frac{1}{N_0} \sum_{s=1}^{N_0} n_k^l(t_s) \right] \left[\frac{1}{N_0} \sum_{s=1}^{N_0} n_j^l(t_s) \right] = \overline{d^{\omega,r}} \overline{n} + (\overline{n})^2. \quad (A5b)$$

Assuming that $\overline{n} \approx 0$, Eq. A3 becomes

$$\overline{\frac{dm_j^l(t)}{dt}} \approx \eta(-\epsilon) \overline{n^2} m_j^l(t) \quad (A6)$$

for the average change to the j^{th} left eye synaptic weight when nonoptimal patterns are presented to the open right eye.

Now when optimal patterns are presented to the responsive and selective open (right) eye and noise to the deprived (left) eye, the cell response falls near θ . At this high level of cell response, ϕ can be approximated by a line with a positive slope ϵ ; that is, $\phi \approx \epsilon(c - \theta)$ (Figure 8). Therefore, the j^{th} left eye synaptic weight modifies as the product of $\epsilon(c - \theta)$ and its input activity $n_j^l(t)$:

$$\frac{dm_j^l(t)}{dt} \approx \eta \epsilon (c - \theta) n_j^l(t). \quad (A7)$$

Using the same averaging procedures and assumptions as for the nonoptimal patterns, the average change to the j^{th} left eye synaptic weight over the optimal open eye patterns becomes

$$\overline{\frac{dm_j^l(t)}{dt}} \approx \eta(\epsilon) \overline{n^2} m_j^l(t). \quad (A8)$$

The closed eye synaptic weights weaken when the open eye receives non-preferred input (A6) and strengthen when the open eye receives preferred input (A8). To produce

the weakening signal (i.e. A6) we assumed that $\phi \approx -\epsilon c$ near 0. However, we are not confined to this choice. In fact,

$$\phi = \begin{cases} -\epsilon c, & c \geq 0, \\ 0, & c < 0, \end{cases} \quad (A9)$$

is also a viable form for ϕ near the origin. In this case Eqs. A1 – A6 still hold for positive responses near the origin. Since $\phi = 0$ for $c < 0$, any responses less than 0 lead to no change in any of the synaptic weights. Let N_{0+} represent the number of iterations where $c \geq 0$ and N_{0-} represent the number of iterations where $c < 0$ ($N_0 = N_{0+} + N_{0-}$). The average change to the j^{th} left eye synaptic weight is simply Eq. A6 weighted by the ratio N_{0+}/N_0 :

$$\overline{\frac{dm_j^l(t)}{dt}} \approx \eta \left(\frac{N_{0+}}{N_0} \right) (-\epsilon) \overline{n^2} m_j^l(t). \quad (A10)$$

Therefore, for cell responses near the origin the closed eye synaptic weights still decrease, but at a rate reduced by N_{0+}/N_0 . Since $N_{0+} \approx N_{0-}$ for random, uniformly distributed noise, the closed eye synaptic weights weaken at half the rate as compared to Eq. A6.

There are limitations, however, on the form of ϕ near the origin. For example,

$$\phi' = \begin{cases} -\epsilon c, & c \geq 0, \\ \epsilon c, & c < 0, \end{cases} \quad (A11)$$

is an example of a function that does not produce a disconnection of the closed eye synaptic weights for responses near the origin. As expected, for the N_{0+} iterations where $c \geq 0$ Eqs. A1 – A6 remain valid. The analysis for the N_{0-} iterations where $c < 0$ is identical to Eqs. A1 – A6 but with $-\epsilon$ replaced by ϵ . Therefore, the average change to the j^{th} left eye synaptic weight after N_0 iterations is

$$\overline{\frac{dm_j^l(t)}{dt}} \approx \eta \left(\frac{N_{0-} - N_{0+}}{N_0} \right) (-\epsilon) \overline{n^2} m_j^l(t). \quad (A12)$$

For random, uniformly distributed noise in this case (i.e. $N_{0+} \approx N_{0-}$) the closed eye synaptic weights would not weaken when the open eye receives non-preferred input. On average they would increase in strength due to the open eye preferred input. Therefore, to guarantee that the closed eye synaptic weights decrease during MD we take $\phi \geq 0$ for $c < 0$.

FIGURE LEGENDS

Figure 1. Cartoon of a cortical neuron receiving LGN input from the left and right eyes to illustrate the theoretical notation. The horizontal lines represent the LGN-cortical fibers and the solid triangles represent their corresponding synaptic contacts. The cell response c is a linear function of the left and right eye LGN-cortical input activities, represented by the vectors d^l and d^r , and the left and right eye synaptic weights, represented by the vectors m^l and m^r . c is obtained by multiplying the LGN activity d_j of each fiber by its corresponding synaptic weight m_j and summing over all of the synapses to the cell.

Figure 2. Illustration of the types of LGN-cortical input used in the model. The top row of this figure represents a horizontal bar of light on the retina (left), a vertical bar of light on the retina (middle) and the retina in the absence of any stimulation (right). In the middle row we illustrate the distribution of activity in a 2-dimensional array of LGN neurons that might arise from these different types of retinal stimulation. The important point of this figure is that different types of retinal stimulation are mapped onto distinct distributions of LGN activity. We call LGN activity elicited when visual contours are presented to the retina "pattern" input to the visual cortex. We call LGN activity that arises in the absence of visual contours "noise" input to the cortex. As illustrated in this figure, the important difference between pattern and noise input is that for the former there are predictable relationships in the activities of the LGN cells, whereas in the latter the activity of one LGN cell is independent of the activity of the other LGN cells. Different patterns that arise from contours of different orientations, for example, are distinguished by different distributions of correlated activity in the LGN cells. The salient features of the LGN-cortical input can be captured in a 1-dimensional array of LGN fibers, as shown in the bottom row. The pure patterns are described mathematically by $d_{\text{peak}} e^{-\gamma(1-\cos\{\frac{2\pi}{\omega}(j-j_\omega)\})} + d_{\text{base}}$, where j denotes the fiber whose activity is being calculated, j_ω is the fiber where the peak activity occurs for pattern ω , d_{base} is the minimum fiber activity in a pattern, d_{peak} is the peak displacement in

activity from d_{base} and γ describes the rate at which the activity falls off with increasing fiber distance from the fiber with peak activity. In the absence of retinal stimulation the “LGN-cortical” input activity to the network (third row, right hand side) is assumed to be randomly distributed about its spontaneous level, represented by the dashed line.

Figure 3. The ϕ function. (A) The two important values of the cell response ($c_a(t)$) are the average level of the spontaneous activity (c_s) and θ above the average spontaneous level ($c_s + \theta$). The essential properties of ϕ (i.e. the negative slope, called ϵ_0 , for values of c_a just above c_s and the positive slope, called ϵ_θ , through $c_s + \theta$) are illustrated by the solid curves. In the simulations we set $\epsilon_0 = -3$ and $\epsilon_\theta = 3$. The dashed lines complete the definition of ϕ in terms of c_a but are not rigidly specified by experiment. (B) Since the departure of the cell response from its spontaneous level is the quantity of interest, ϕ in Eq. 13 is defined in terms of $c(t)$ which equals $c_a(t) - c_s$.

Figure 4. A simulation of NR for a cortical cell receiving one set of LGN-cortical afferent fibers. The 3-dimensional figure shows the evolution of the cell’s response to different input patterns (stimulus “orientations”) as a function of time, or iteration number. Cross-sections through this figure at a given iteration can be viewed as the tuning curve of the cortical neuron to stimuli of various orientations. There are N_p patterns (stimulus “orientations”) in the training and testing set (Eq. 22); to produce the continuous curves in the 3-dimensional graphs the cell’s responses to the N_p patterns at different times are connected in a smooth manner. The graded color scale (upper left) is the legend for the strength of the response: red corresponds to the maximum response, purple corresponds to the minimum response and blue is at the level of spontaneous activity. This same legend applies to all of the 3-dimensional graphs in Figures 6 through 13; therefore, the strength of the cell response in one figure can be directly compared to the cell response in any other figure. To illustrate how responses above θ increase in strength and those below θ decrease in strength, three slices through the 3-dimensional graph are illustrated to the right of the figure. The dashed white horizontal line represents the cell’s level of spontaneous activity and the solid white line represents the value of θ . As the tuning

curve becomes more selective, θ increases and eventually stabilizes the synaptic weights.

Figure 5. The sign and magnitude of the change to the j^{th} LGN-cortical fiber (dm_j/dt) for different values of the fiber activity (d_j) and the cell response (c). Notice that the relative sizes of the four regions change as θ (represented by the arrow) moves.

Figure 6. A simulation of normal rearing with binocular input. The initial state for this simulation was randomized synaptic weights near 0. It ran for 200,000 iterations. Note that the cell response becomes stable, binocular and selective. See Figure 4 for response legend.

Figure 7. A simulation of monocular deprivation. The initial state for this simulation was the stable, binocular, selective equilibrium state achieved during normal rearing (Figure 6). This simulation ran for 200,000 iterations. Note the loss of responsiveness of the closed eye. See Figure 4 for response legend.

Figure 8. The average change to the j^{th} left eye synaptic weight (i.e. m_j^l) when the left eye set of LGN-cortical fibers carries noise and θ is sufficiently far from 0. For cell responses scattered around 0 the average change to m_j^l is given by Eq. 23a, while for cell responses scattered around θ the average change to m_j^l is given by Eq. 23b. Note that $\overline{[n_j^l]^2} = \overline{n^2}$ for all j .

Figure 9. A simulation of reverse suture. The beginning state for this simulation was the stable equilibrium state after monocular deprivation (Figure 7). This simulation ran for 200,000 iterations. Note the loss of responsiveness of the newly closed eye before the recovery of responsiveness of the newly opened eye. See Figure 4 for response legend.

Figure 10. A simulation of strabismus. The initial state was the stable, selective equilibrium state after normal rearing (Figure 6). This simulation ran for 200,000 iterations. Note that the cell response becomes monocular. See Figure 4 for response legend.

Figure 11. A simulation of binocular deprivation. The initial state was the stable,

selective equilibrium state after normal rearing (Figure 6). This simulation ran for 200,000 iterations. Note that on the same timescale as monocular deprivation (Figure 7) the loss of responsiveness is not as severe during binocular deprivation. See Figure 4 for response legend.

Figure 12. The same binocular deprivation simulation as illustrated in Figure 11, but graphed over 2,000,000 iterations. For longer such simulations the cell loses its selectivity but retains some binocular responsiveness. See Figure 4 for response legend.

Figure 13. A simulation of recovery after a period of monocular deprivation. This simulation ran for 200,000 iterations. Note that there is a recovery since the patterned input to the two eyes is correlated. See Figure 4 for response legend.

Figure 14. Peak cell response versus iteration for 200,000 iterations of the normal rearing, monocular deprivation, reverse suture, strabismus, binocular deprivation and recovery simulations. These graphs represent the evolution of the left and right eye peak cell responses taken from Figures 6, 7, 9, 10, 11 and 13, respectively. The dashed line is at the cell's average spontaneous level ($c = 0$). See Figure 4 for response legend.

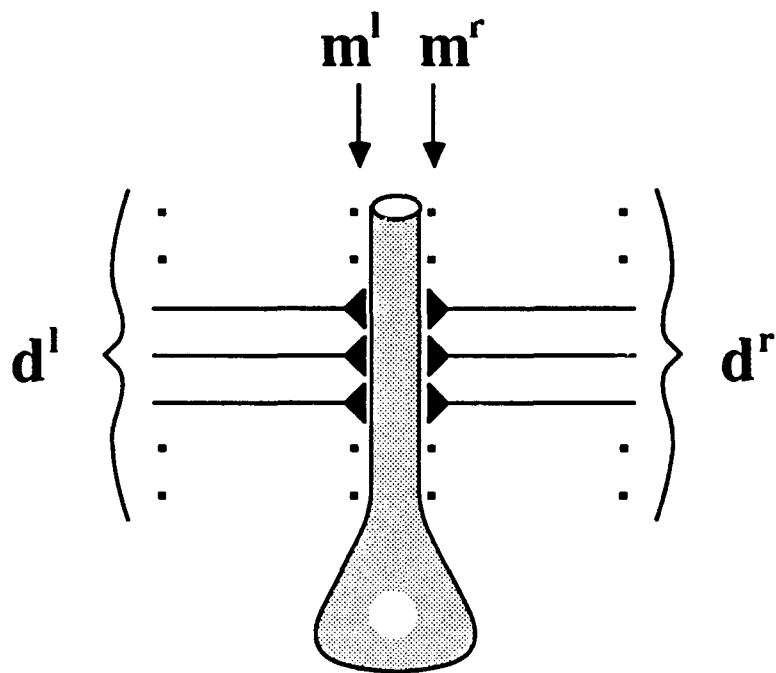
TABLE LEGENDS

Table 1. List of Definitions.

Table 2. List of Parameters and Theoretical Constraints.

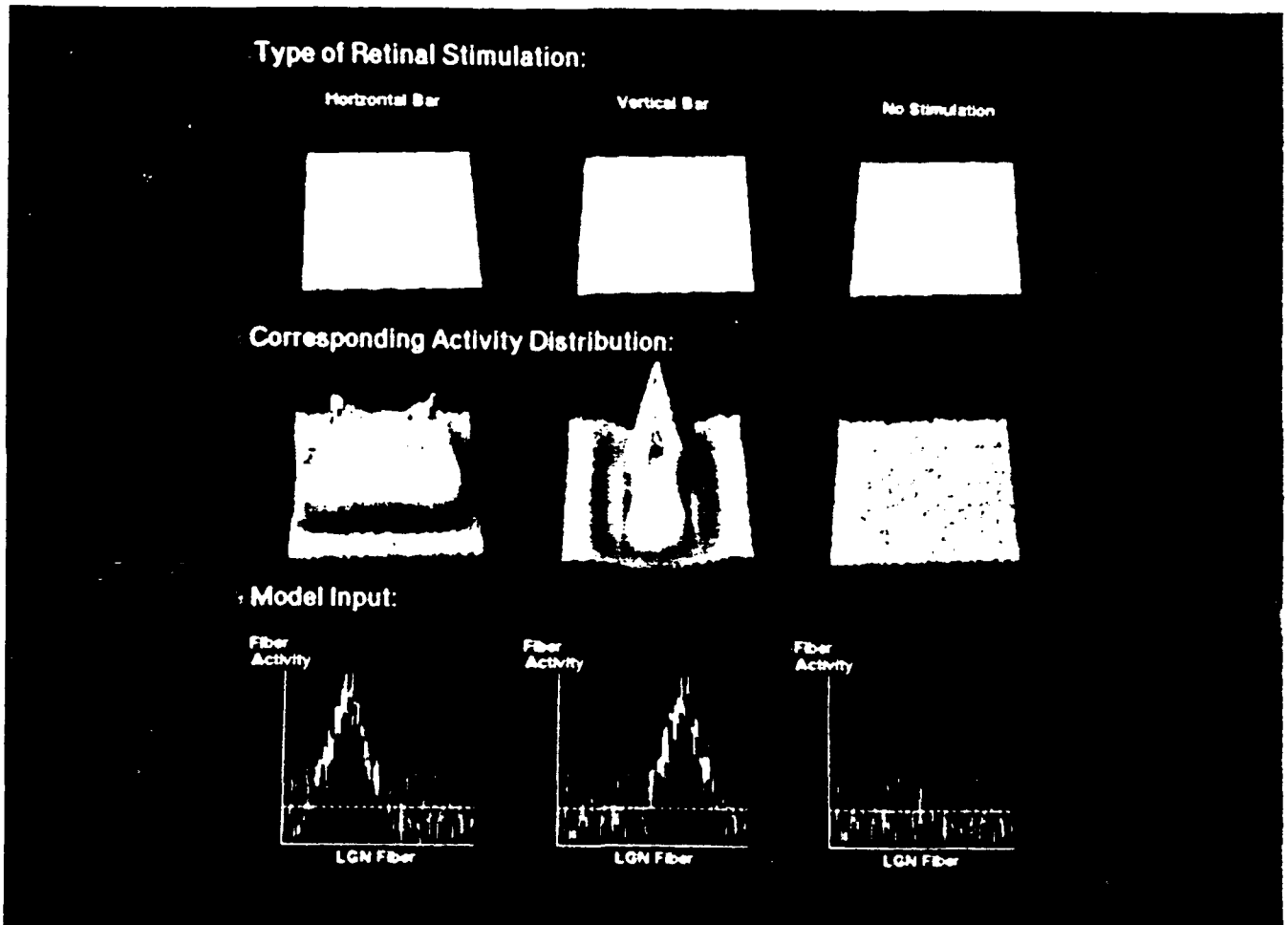
Table 3. Sensitivity of Results to Parameter Values. The value of the parameter either has a critical effect on the results of the simulation (++), affects the outcome of the simulation but is not critical (+), or does not affect the outcome of the simulation (0). Blank spaces indicate that the effect of the parameter on the simulation has not been studied in detail.

Clothiaux, Bear and Cooper
Figure 1
Top

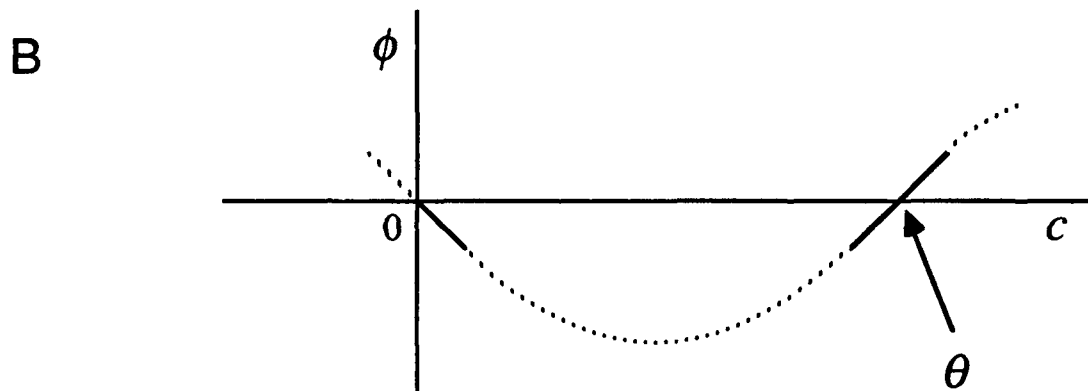
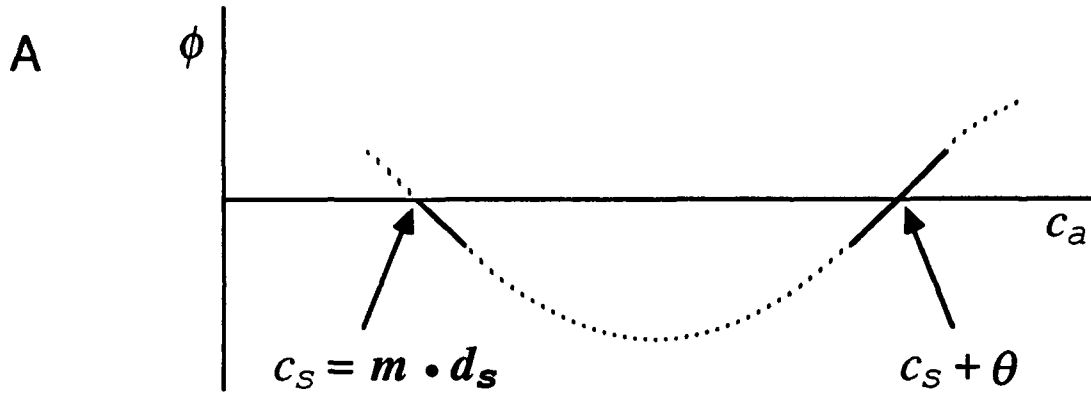


$$c = (m^l \cdot d^l) + (m^r \cdot d^r)$$

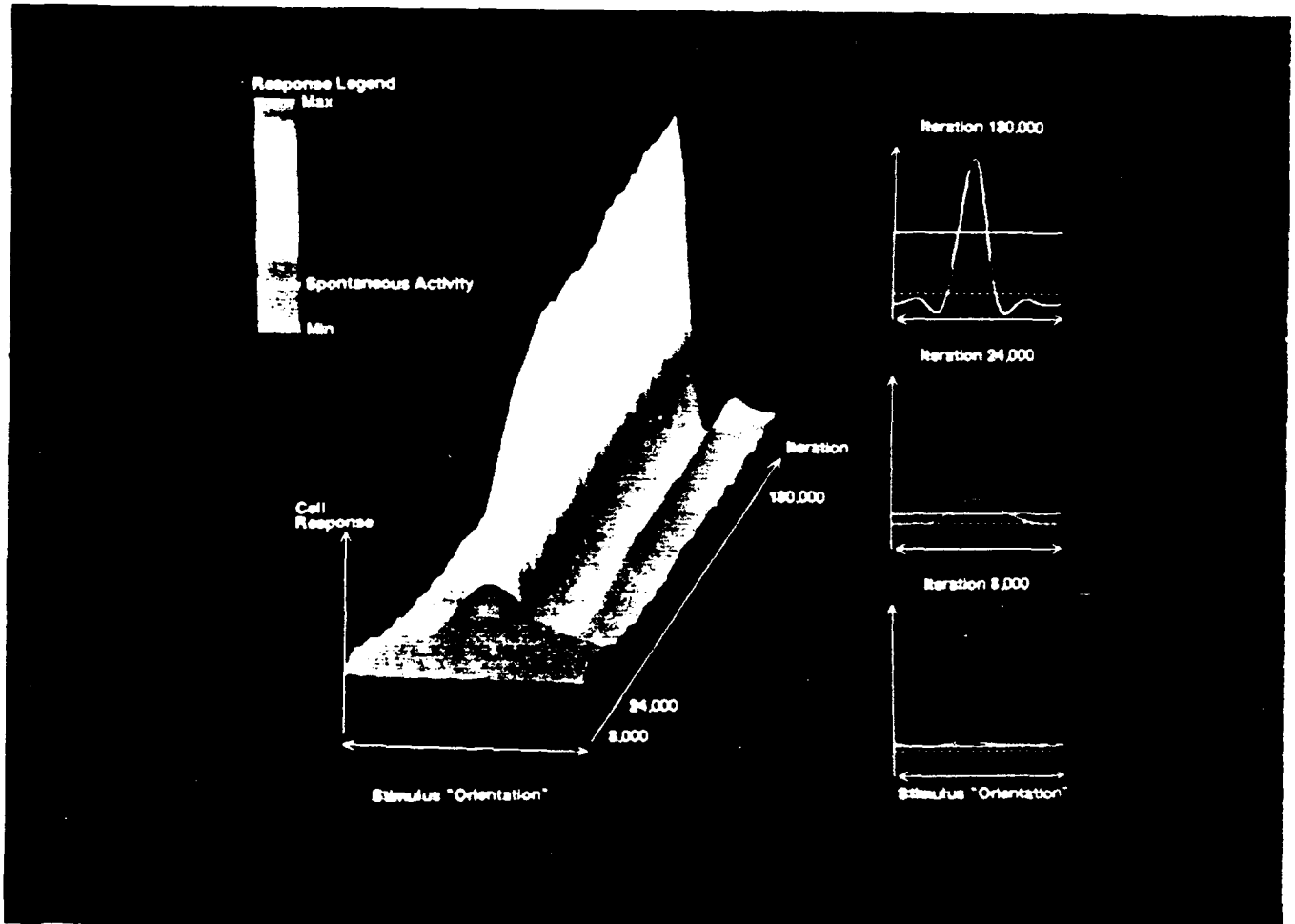
Clothiaux, Bear and Cooper
Figure 2
Top



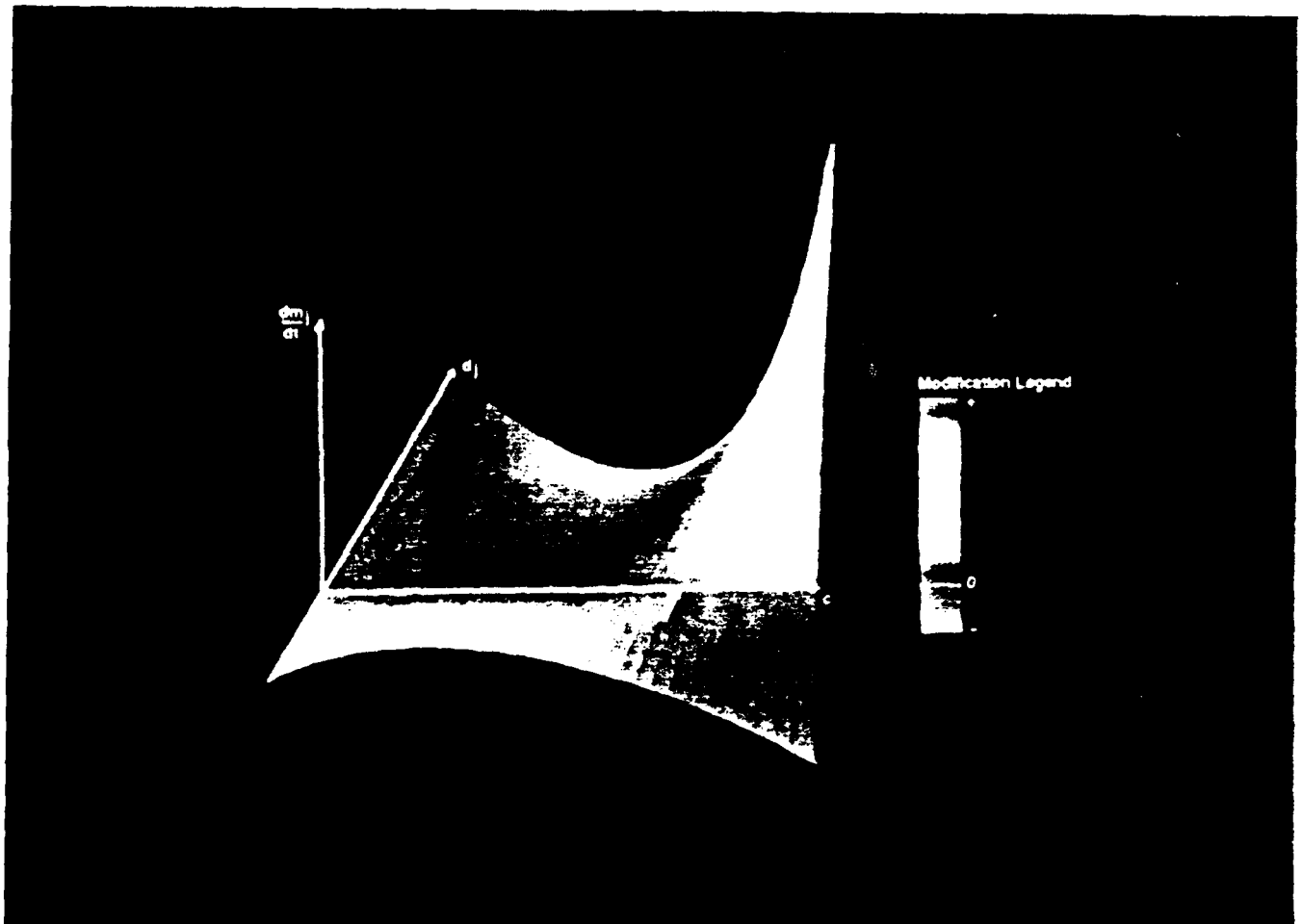
Clothiaux, Bear and Cooper
Figure 3
Top



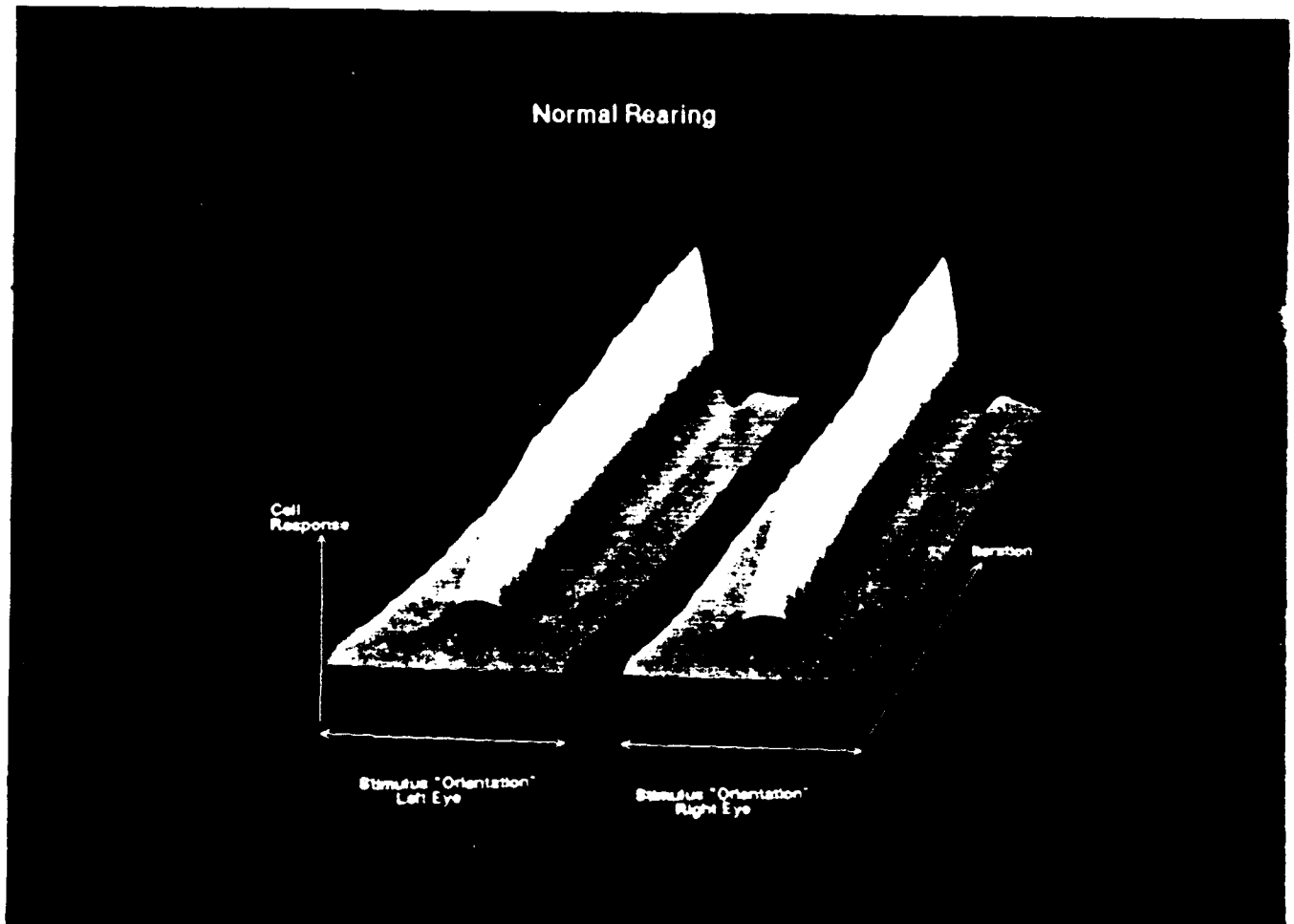
Clothiaux, Bear and Cooper
Figure 4
Top



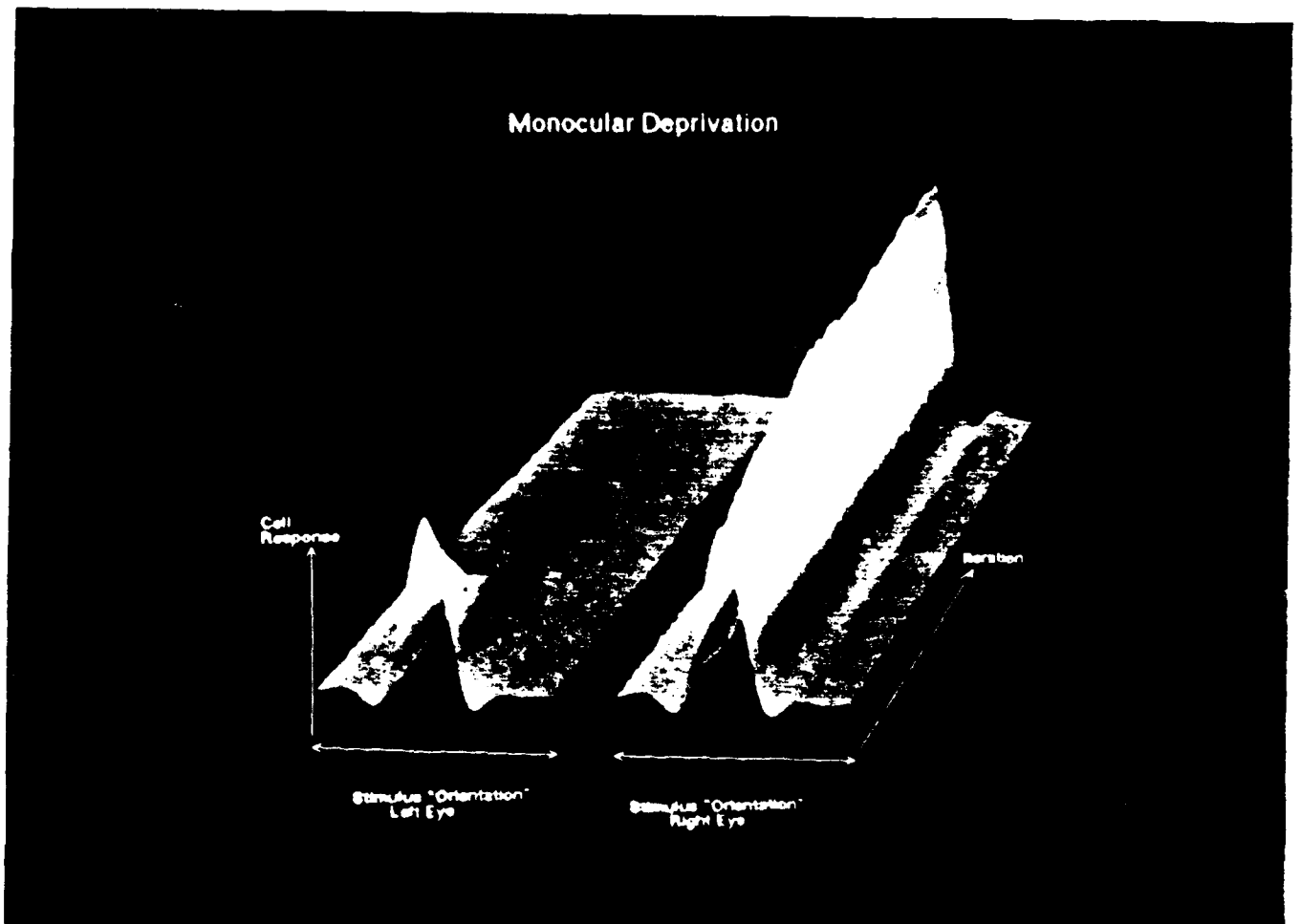
Clothiaux, Bear and Cooper
Figure 5
Top



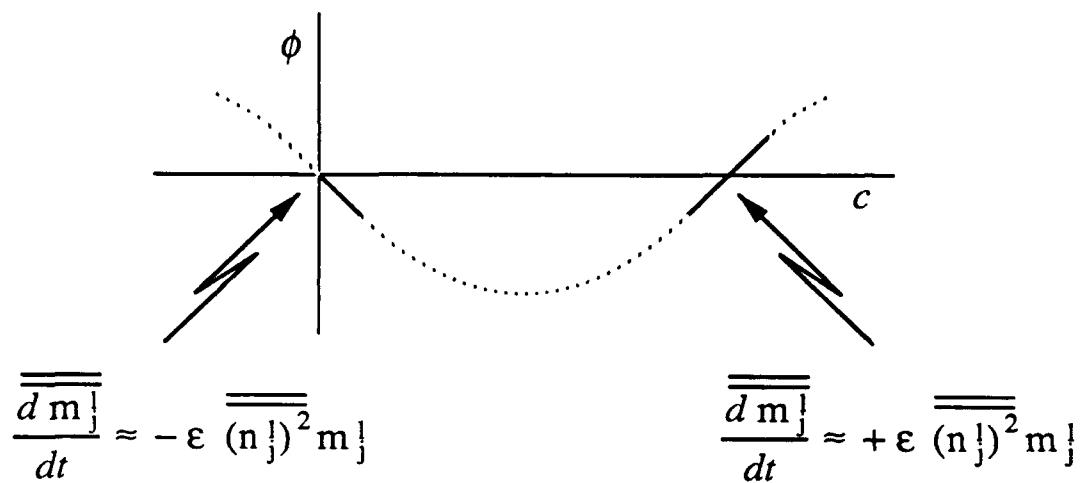
Clothiaux, Bear and Cooper
Figure 6
Top



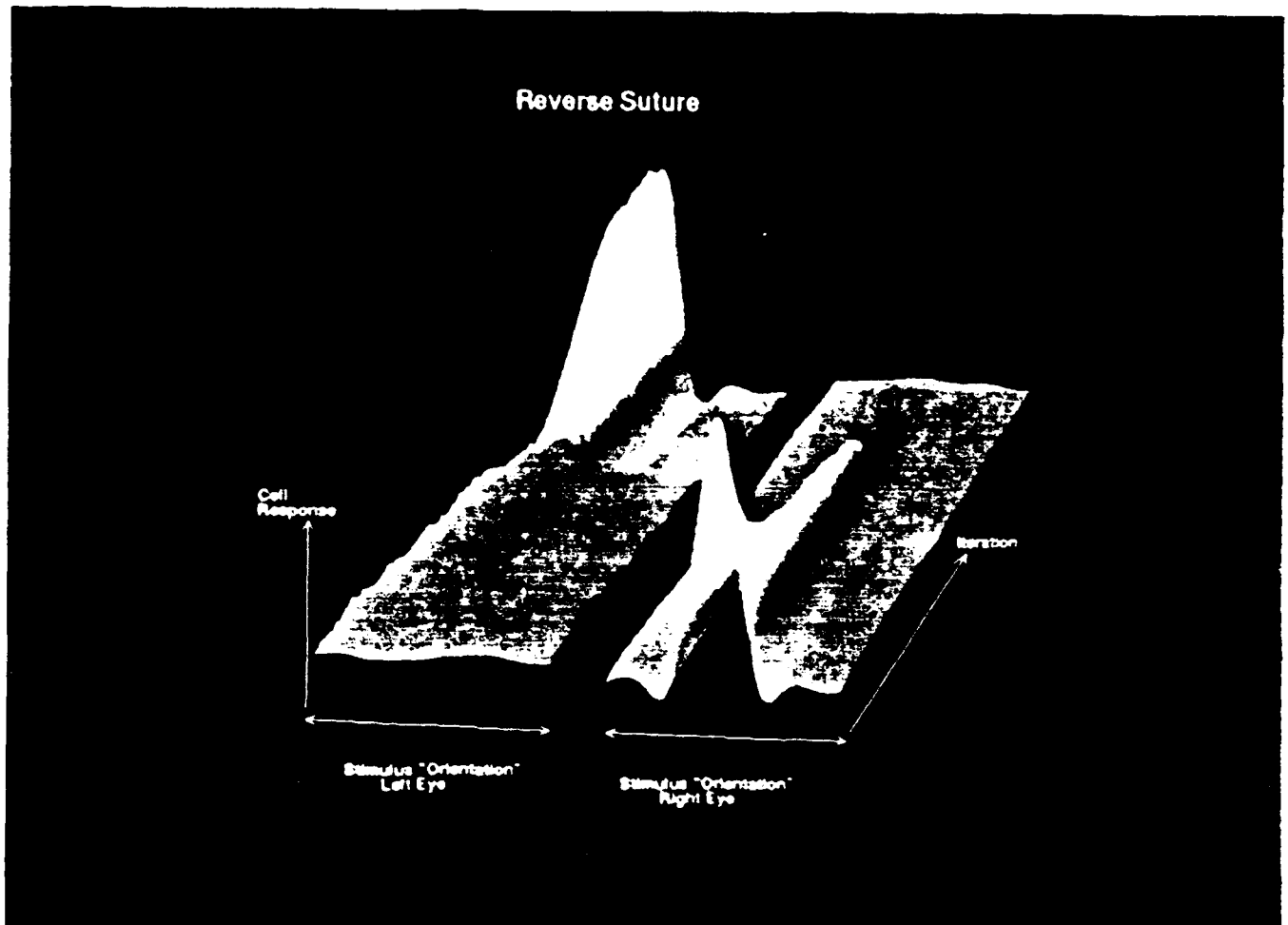
Clothiaux, Bear and Cooper
Figure 7
Top



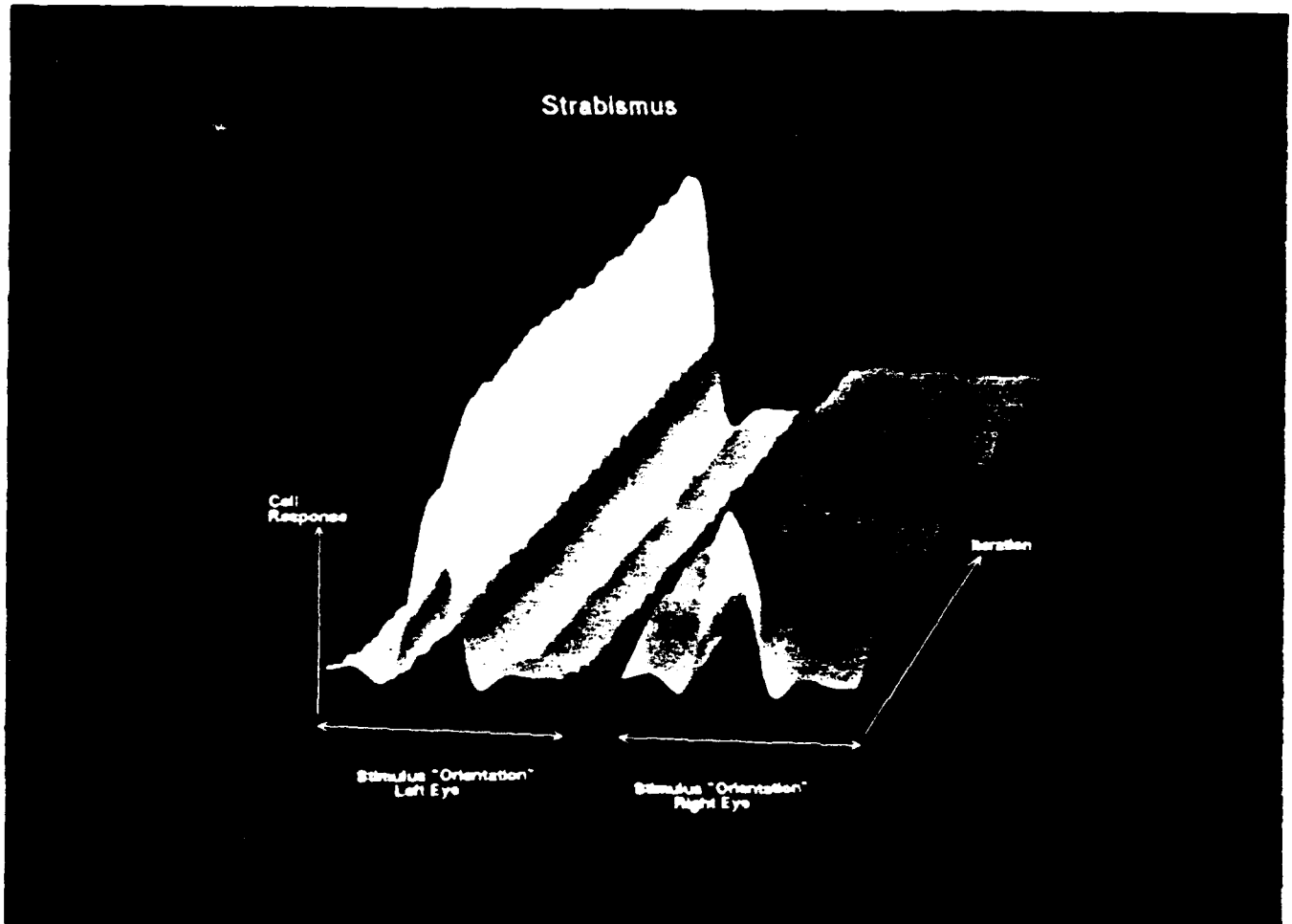
Clothiaux, Bear and Cooper
Figure 8
Top



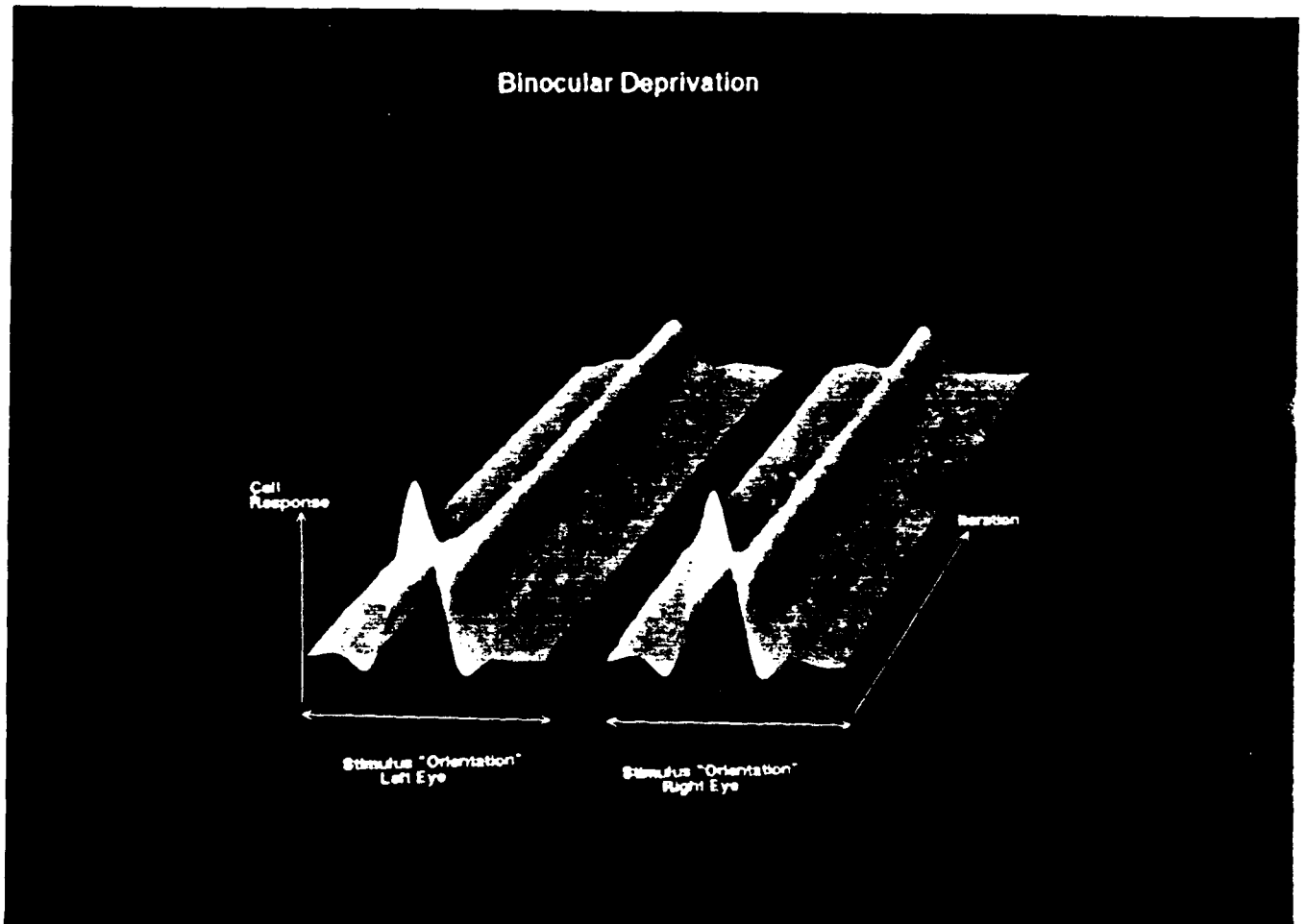
Clothiaux, Bear and Cooper
Figure 9
Top



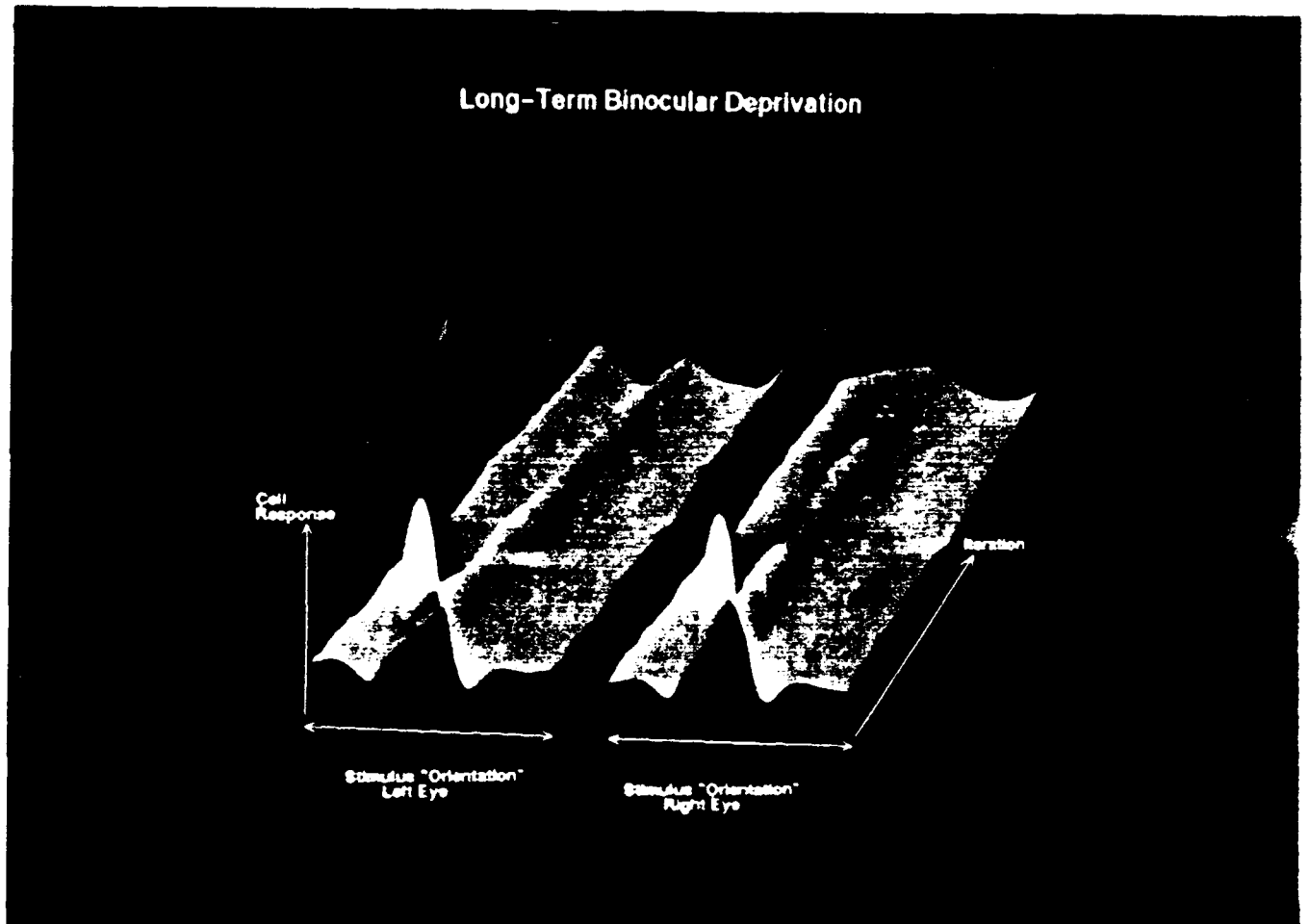
Clothiaux, Bear and Cooper
Figure 10
Top



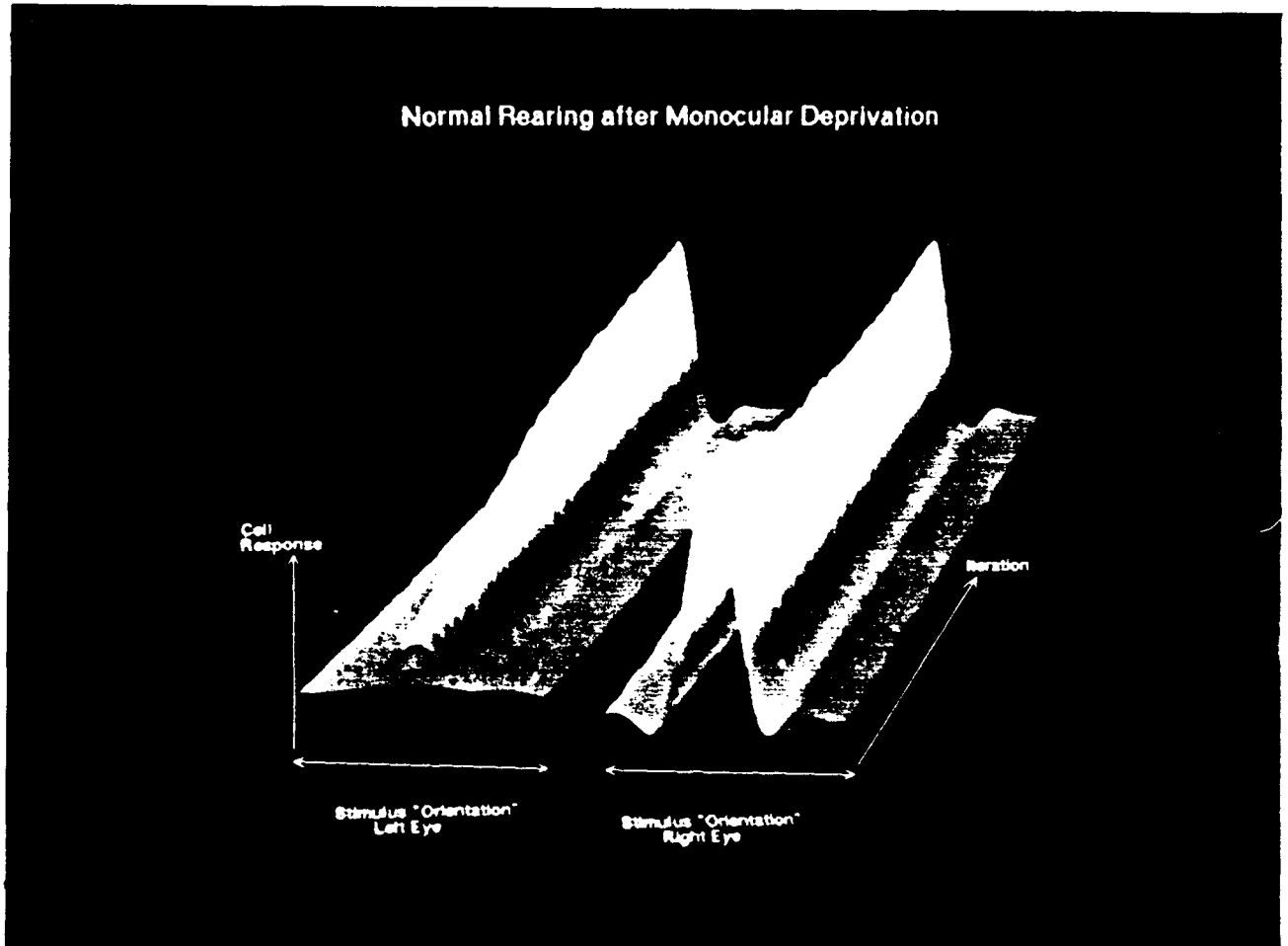
Clothiaux, Bear and Cooper
Figure 11
Top



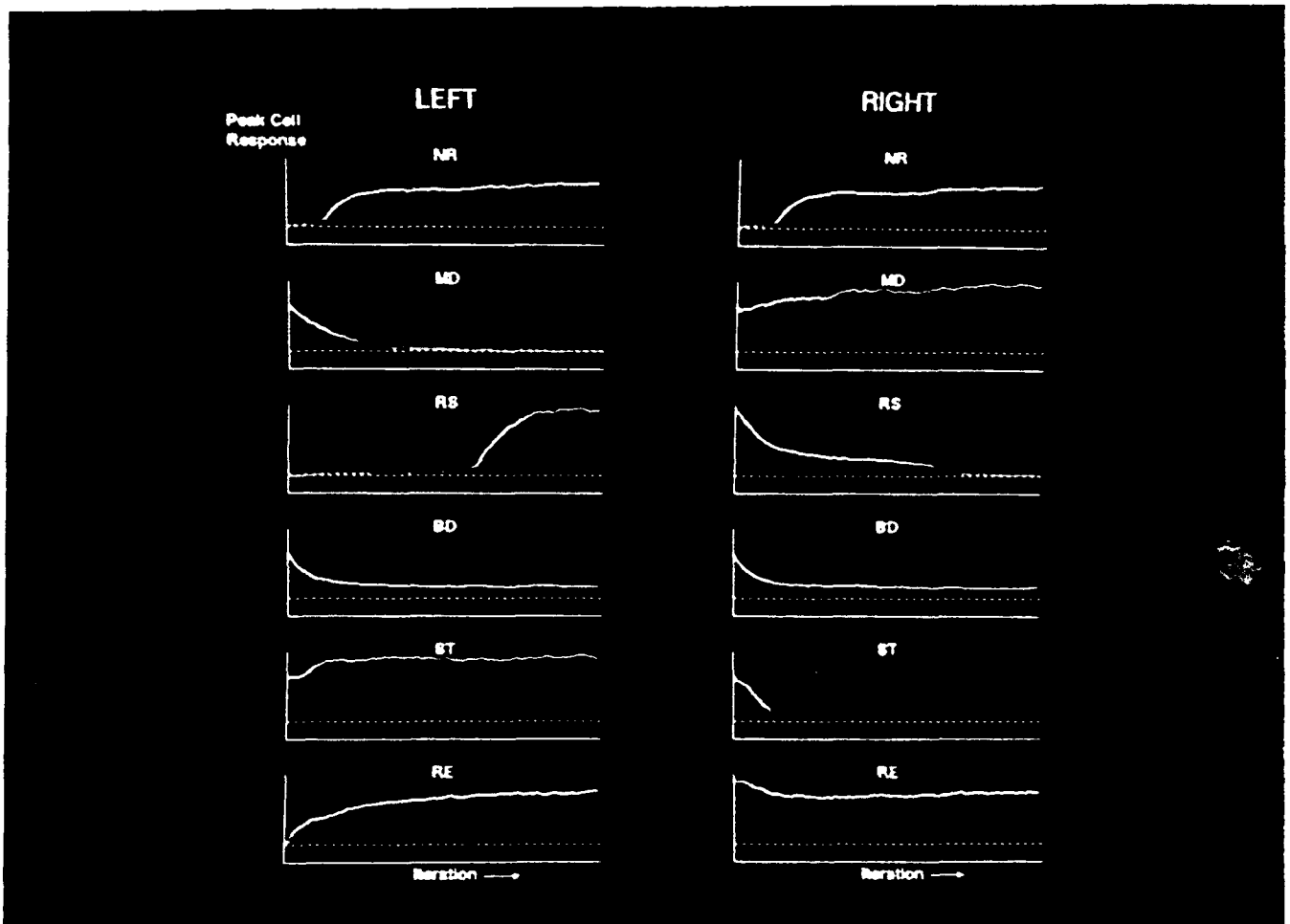
Clothiaux, Bear and Cooper
Figure 12
Top



Clothiaux, Bear and Cooper
Figure 13
Top



Clothiaux, Bear and Cooper
Figure 14
Top



Clothiaux, Bear and Cooper
Table 1
Top

“Spontaneous” Level of the Cell Response:

$$c_s(t) = m(t) \cdot d_s = m^l(t) \cdot d_s^l + m^r(t) \cdot d_s^r,$$

where $d_s^l = d_s^r =$ Spontaneous activity of the LGN-cortical afferent fibers.

The Actual Level of the Cell Response:

$$c_a(t) = m(t) \cdot d_a(t) = m^l(t) \cdot d_a^l(t) + m^r(t) \cdot d_a^r(t),$$

where $d_a(t) =$ Actual activity in the LGN-cortical afferent fibers.

The Cell Response Measured with Respect to the Spontaneous Level with non-LGN Noise Superimposed:

$$c(t) = c_a(t) - c_s(t) + c_{\text{noise}}(t) = m^l(t) \cdot d^l(t) + m^r(t) \cdot d^r(t) + c_{\text{noise}}(t),$$

where $d^l(t) = d_a^l(t) - d_s^l$, $d^r(t) = d_a^r(t) - d_s^r$ and $c_{\text{noise}}(t)$ represents non-LGN noise.

Components of $d^l(t)$ and $d^r(t)$ (Patterned Input):

$$d_j^l(t) = d_j^{\omega,l} + n_j^l(t) = d_{a,j}^{\omega,l} - d_s + n_j^l(t),$$

$$d_j^r(t) = d_j^{\omega,r} + n_j^r(t) = d_{a,j}^{\omega,r} - d_s + n_j^r(t),$$

where ω represents one of the N_p patterns of activity.

Components of $d^l(t)$ and $d^r(t)$ (Noise Input):

$$d_j^l(t) = n_j^l(t),$$

$$d_j^r(t) = n_j^r(t).$$

Rule for Synaptic Modification:

$$\frac{dm(t)}{dt} = \eta \phi(c(t), \theta(t)) d(t),$$

where

$$\theta(t) = \frac{\overline{c_a(t)}^P}{c_0},$$

$$\overline{c_a(t)} = \frac{1}{\tau} \int_{-\infty}^t c_a(t') e^{-\frac{(t-t')}{\tau}} dt'.$$

Clothiaux, Bear and Cooper
Table 2
Top

Parameter	Significance	Theoretical Constraint	Value Used
N_{gl}	Number of LGN-cortical input fibers from one eye	None	12
N_p	Number of training patterns	None	12
$d_{a,j}^{\omega,l(r)}$	ω^{th} input pattern*	None	$d_{peak} = 1.0$ $d_{base} = d_s$ $\gamma = 4.0$
d_s	Level of spontaneous activity	None	$d_s = 5.0$
\bar{n}	Average value of the noise input along the LGN-cortical fibers	None	0
$\overline{n^2}$	Average of the square of the noise input along the LGN-cortical fibers	None	0.03
$m_j^{l(r)}(0)$	Starting values of the synaptic weights for normal rearing	None	0.0 to 0.1
$\overline{c_{noise}}$	Average value of the non-LGN postsynaptic noise	None	0
$\overline{c_{noise}^2}$	Average of the square of the non-LGN postsynaptic noise	None	33.3
η	The modification step size	Upper bound that decreases with increasing τ	0.005
τ	Time constant in the definition of θ	Must lead to an adequate sampling of inputs	1000
p	Nonlinearity in the definition of θ	$p > 1$	2
c_0	Normalization constant in the definition of θ	None	50

* See legend of Figure 2

Clothiaux, Bear and Cooper
 Table 3
 Top

Parameter	NR	MD	RS	BD	ST	RE
N_{gl}	0	0	0	0	0	0
N_p	0	0	0	0	0	0
$d_{a,j}^{\omega,l(r)}$	0	0	0	0	0	0
d_s	0	0	++	++	0	0
\bar{n}	0	+	+	++	0	0
$\overline{n^2}$	0	++	++	++	0	++
$m_j^{l(r)}(0)$	0	0	0	0	0	0
$\overline{c_{noise}}$						
$\overline{c_{noise}^2}$	+	+	+	++	+	0
η	++	0	0	0	0	0
τ	++	0	++	++	0	0
p	++					
c_0	+					